Master's Thesis
석사 학위논문

# The Study on the Quantum Dot Sensitized Solar Cells

Min Ji Lim (임 민 지 林 珉 知)

Department of Energy Systems Engineering
에너지시스템공학전공

**DGIST**

**2014**

Master's Thesis
석사 학위논문

# The Study on the Quantum Dot Sensitized Solar Cells

Min Ji Lim (임 민 지 林 珉 知)

Department of Energy Systems Engineering
에너지시스템공학전공

**DGIST**

**2014**

# The Study on the Quantum Dot Sensitized Solar Cells

Advisor : Professor Jong-Soo Lee

Co-advisor : Professor Jeong Nak Cheon

by

Min Ji Lim

A thesis submitted to the faculty of DGIST in partial fulfillment of the requirements for the degree of Master of Science in the Department of Energy Systems Engineering. The study was conducted in accordance with Code of Research Ethics[1]

2013. 11. 26

Approved by

Professor (Advisor) Jong Soo-Lee ( Signature )

Professor (Co-Advisor) Nak Cheon Jeong ( Signature )

[1] Declaration of Ethical Conduct in Research**:** I, as a graduate student of DGIST, hereby declare that I have not committed any acts that may damage the credibility of my research. These include, but are not limited to: falsification, thesis written by someone else, distortion of research findings or plagiarism. I affirm that my thesis contains honest conclusions based on my own careful research under the guidance of my thesis advisor.

# The Study on the Quantum Dot Sensitized Solar Cells

Min Ji Lim

Accepted in partial fulfillment of the requirements for the degree of Master of Science.

Head of Committee _____(인)
Prof. Jong-Soo Lee
Committee Member _____(인)
Prof. Nak Cheon Jeong
Committee Member _____(인)
Prof. Youngu Lee

MS/ES
201224017

임 민 지. MinJi Lim. The study on the Quantum Dot Sensitized Solar Cells Department of Energy Systems Engineering. 2014. 50p. Advisors Prof. Lee, Jong-Soo. Prof. Co-Advisors. Lee, Young Gu, Jeong, Nak Cheon.

**Abstract**

The Quantum Dot Sensitized Solar Cells (QDSSCs) using Pt as its counter electrode and poly-sulfide redox shuttle have problems on the low QD's regeneration speed and high over potential. Sulfur compounds induce a poisoning effect because it was chemisorbed onto the Pt surface. It leads to poor charge transfer rate ($Sn^{2-}+e^{-}\rightarrow nS^{2}$) at the counter electrode and high over potential for the reduction reaction. The $Cu_2S$ was proposed as an ideal counter electrode materials for higher performance QDSSCs due to their higher electrical catalytic activity and stability. In this study, $Cu_2S$ nanocrystals (NCs) are proposed as counter electrode. At the result of, the efficiency of QDSSCs using $Cu_2S$ NCs as counter electrode is 0.2% higher than that of using the Pt counter electrode. In addition, The rate of reduction of the $Cu_2S$ NCs capped with organic ligands replaced with $Na_2S$ (Inorganic) ligands lead to significantly increase. It is demonstrated that the rate of reduction process with $Na_2S$_capped $Cu_2S$ NCs counter electrode was more 3 times higher than that of organic_ capped $Cu_2S$ NCs counter electrode. Electrochemical impedance spectra (EIS) also confirmed much less resistance by using $Na_2S$ capped counter electrode. Finally, we also studied on the effects of nanomaterials and surface modification on the operation of QDSSCs using photoanode materials like CdSe which synthesized by SILAR and hot-temperature injection method.

Keywords: Quantum dot sensitized solar cell, $Cu_2S$ nanocrystals, SILAR, colloidal nanoparticles method, ligand exchange

# Contents

# List of tables

# List of figures

# 1. Introduction

The most widely used energy sources currently are fossil fuels. The renewable energy has become a hot topic since fossil fuels are running out and the awareness of environmental damage is increasing. It is now possible to make hydrothermal energy, wind energy, and solar energy available for the environment. Among a variety of energy, the solar energy is the most promising energy. Solar energy makes use of light and the radiant heat from the sun striking the earth. A solar cell (Photovoltaic cell), which is the smallest semiconductor device, converts solar energy directly to electricity [2].

First generation solar cells, were based on the crystalline silicon, have been widely used. They have over 20% efficiency nowadays, whereas the semiconductor industry has toxic chemicals and the cost is very expensive. DSSCs (Dye sensitized solar cells) were invented by Michael Gratzel in 1991. They have drawn attention as an alternative to silicon solar cells because they are easy process, have good and long-term stability, and are made from low cost materials. In addition, they are based on a photo electrochemical solar cell unlike other types of solar cells (thin film solar cell, organic photovoltaic cell). Dyes for sensitizers, have disadvantage, they are not able to absorb light at the wavelength above the band gap. Also dyes can only adsorb in visible region. In substitute for Dye, Quantum Dots (QDs) are highly promising sensitizers[3] [4] because they can tune the band gap by size control, which can be used to match the absorption spectrum to the spectral distribution of solar light. Compared to other materials, it has higher exciton coefficient [5] [6]. Therefore QDs were used to utilize a single energy photon to produce multiple electron-hole pairs. This is called as phenomena of multiple exciton generation (MEG) [7] [8]. Additionally QDs has large intrinsic dipole moment inducing rapid charge separation [9] [10]. Combining desirable features; the efficiency

raise their theoretical maximum efficiency above the Shockley Queisser limit of 31%. The principle of Quantum Dot Sensitized Solar Cells (QDSSCs) is same as DSSCs, in which photo excited electrons in QDs are injected into the nanocrystalline $TiO_2$ semiconductor from the excited QDs.

Computation for maximum efficiency of QDSSCs results about 31%, but now the best recorded is only about 10%. The reason for poor efficiency can be attributed to charge recombination. It is related electron intercept, back electron transfer which occur interface between photoanode and electrolyte. Additional problem is electrical catalytic activity between the electrolyte and the counter electrode. This paper is mainly focused on improving electrical catalytic activity at the counter electrode using liquid electrolyte (poly sulfide solution) for high performance of QDSSCs.

There are two strategies to sensitize QDs onto the wide band gap nanocrystalline semiconductor ($TiO_2$, ZnO): (1) direct growth of the semiconductor QDs on the electrode surface by chemical reaction of ionic species using the methods of chemical bath deposition (CBD) [11] [12] or successive ionic layer absorption and reaction (SILAR) [13] [14] (2) directly QDs are adsorbed(DA) on the semiconductor surface. pre-synthesized colloidal QDs attached to the electrode material by linker group (3-MPA, EDT) [15] [16] [17] [18] [19]. This method can control the composition and size, however, it leads to lower short circuit current ($J_{sc}$) because of the length of the functional group.

In the case of DSSCs, Pt is a commonly used counter electrode because of its good electro catalytic activity and long term stability. Polysulfide sulfide reduction reaction is depicted as $Sn^{2-}+e^{-}\rightarrow nS^{2-}$. They are beneficial to the stability for QDSSCs; however it is hard to attain the higher electrical catalytic activity [20]. The chemisorbed sulfur compounds at Pt counter electrode effect hurdle charge transfers from electrolyte to the counter electrode.

Therefore high over potential are applied for reduction reaction, promoting back electron transfer at the photoanode.

The best advantage of metal-chalcogenide electrodes, for example $Cu_2S$, CoS, and PbS exhibits higher electrical catalytic activity when used in conjunctions with photoanode. This counter electrode expects higher efficiency and higher fill factor. Many researchers adopt the method that exposes foils of Cu, Co, or Pb to sulfide solution to obtain interfacial layer of metal sulfide. The occurring problems suffer from continual corrosion and mechanical instability.

This thesis focused on the $Cu_2S$ NCs counter electrode. NCs have a higher surfaces compared to foil and the size is above c.a. 4-5nm. To make proper counter electrode, we consider two factors. [21] (1) Adhesion properties between the FTO substrate and metal sulfides and (2) The size effect of metal sulfides.

A $Cu_2S$ counter electrode was made via drop casting method. This method was adopted to cover a monolayer on the FTO substrates. Furthermore, heat treatments are needed to induce crystallinity to up the electrical catalytic activity. We confirmed when the photoanode in conjunction with $Cu_2S$ counter electrode was slightly exceeded compared to Pt counter electrode.

Copper (II) sulfides ($Cu_2S$) NPs were synthesized via solution, which enables mass production of electrode materials and easy fabrication. The final NPs have distinct surface charges by using magic solution. Magic solution allows facial deposition through electro assembly of nanoparticles.

Photoanode was made by SILAR, Colloidal Nanoparticles Method. The efficiency was compared as method making photoanode. MPA ligands, which has carboxyl group (-COOH) that attaches to $TiO_2$ and thiol group (-SH) that attaches to the QDs, was employed to link QDs and $TiO_2$. SILAR process that the semiconductor film was immersed in the cation

solution, and then was immersed anion solution, alternatively, to grow the target QDs. At result, the SILAR method has a much higher performance. Below the results shows the different amount absorbance between SILAR and Colloidal Nanoparticles method; SILAR process has 0.6% higher performance than colloidal nanoparticles method. In case of colloidal nanoparticles method, the spatial charge separation especially causes lower current than $4mA \cdot cm^{-2}$ under one sun illumination.

We did electrochemical study such as linear sweep voltammetry (LSV), cyclic voltammetry (CV) and Electrochemical Impedance Spectroscopy (EIS) to investigate the result from inorganic ligands exchange affect [22]. According to talaphin paper, the results indicate electron mobility with $Na_2S$ capped $Cu_2S$ NCs are three times faster than organic capped $Cu_2S$ NCs. In addition, the interfacial resistance is significantly decreased. However the performance of solar cell is almost same when in conjunction with the inorganic capped $Cu_2S$ NCs compared to organic capped solar cells via ex-situ method. Except for the reduction reaction process, electron injection, charge separation, and charge recombination are considered determining the power conversion efficiency.

# 2. Overview of Solar Energy

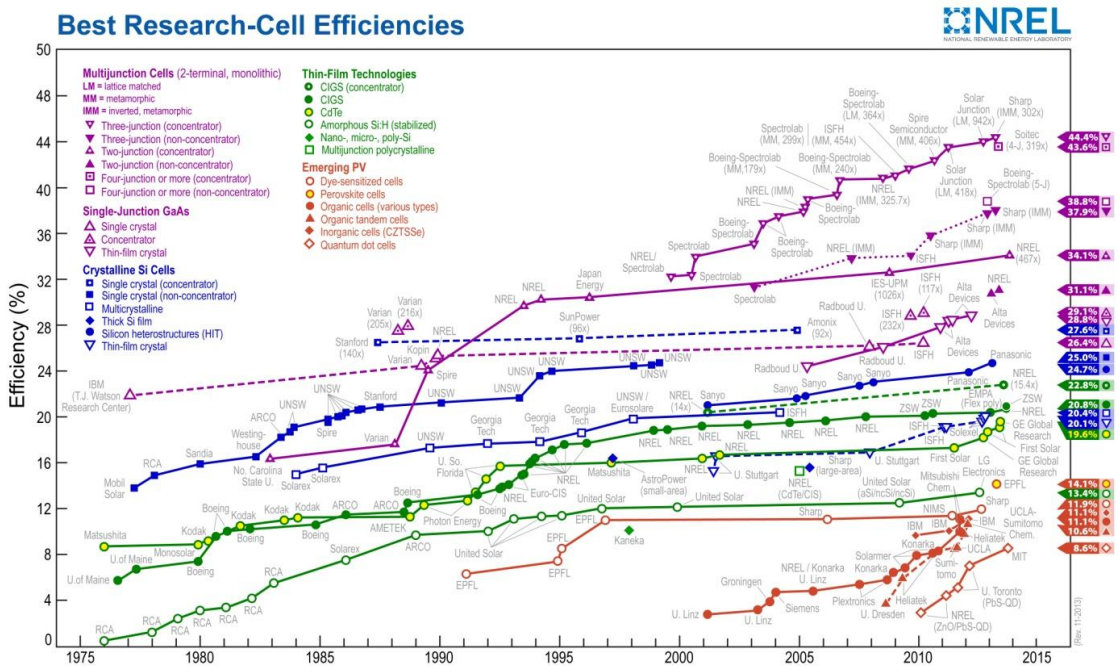


Fig 2.1 Power conversion efficiency depending on a variety of cells [23]

Above the chart shows the best research cell efficiencies depending on a variety of solar cells. Silicon based solar cells are over the 50% on the market. Except for silicon based solar cells, there are a variety of solar cells such as thin film solar cells, CdTe solar cells, organic photo voltaic cells, and DSSCs.

2nd generation solar cells

Thin film solar cells

Thin film solar cells are comprised of amorphous silicon solar cells, CdTe solar cells, Copper-Indium-Gallium-Selenium (CIGS) solar cells. Thin film materials are usually made by physical or chemical deposition techniques, which can be possible for large areas and fast t

output process. Good thin film materials should be low cost, nontoxic, robust, and stable. They should adsorb light more strongly than silicon. Higher absorption reduces the cell thickness.

Amorphous solar cells

Compared to the techniques of amorphous solar cells, it is relatively simple and inexpensive. For a given layer of thickness, amorphous silicon absorbs much more energy than crystalline silicon. Amorphous semiconductor contains intrinsic defects which increase the density of traps and recombination areas. It is used for long minority-carrier diffusion lengths. This principle leads that the collection rate of electrons moving from the n- to p-type contact is better than holes moving from p- to n- type contact. This reason is that amorphous silicon has much higher energy than crystalline silicon solar cells (about 2.5 times).

CdTe solar cells and I-III-VI ternary compounds

Silicon solar cells have a proper band gap for photovoltaic cells. It can be extended to compound semiconductor such as Cadmium telluride (CdTe) solar cells, and *I-III-VI* ternary compounds solar cells. This two type solar cells adopt with an n-type CdS emitter in order to minimize QE losses in the emitter. This heteronjuctions interfaces makes additional defects which act as recombination centers and reduce the open circuit voltage. It allows a barrier in the conduction band, impending electron collection. It can improve contact with aubstrate and reduce losses due to surface recombination in the emitter.

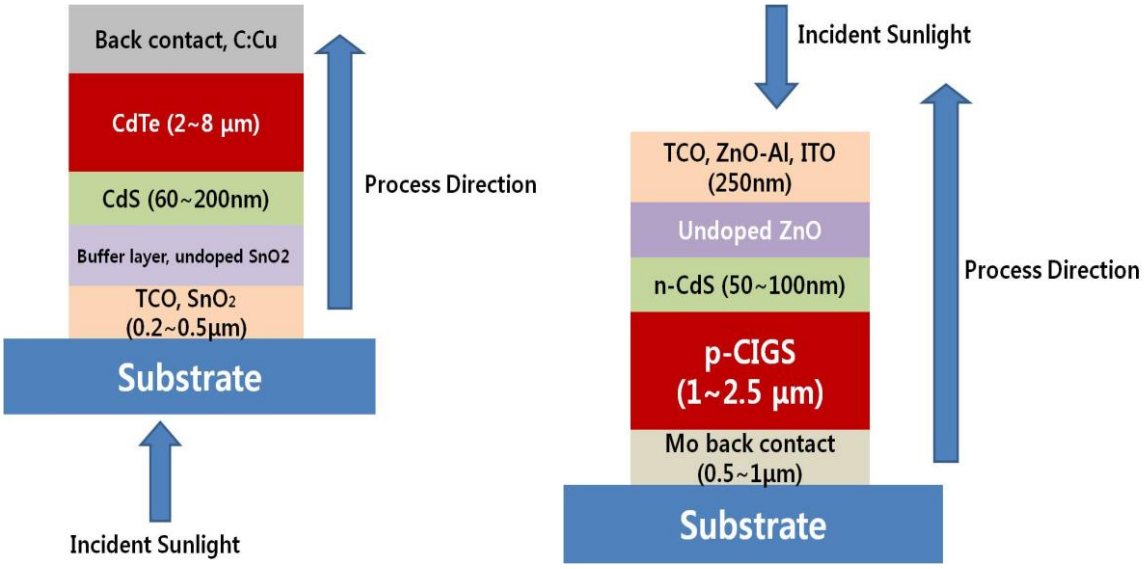


Fig 2.2 The structure of CdTe thin film solar cells (left), CIGS thin film solar cells (right)[1].

3rd generation solar cells

Organic Photovoltaic Cells and Dye sensitized solar Cells

Fig 2.3 Practical example of OPV

Organic photovoltaic cells

The best advantage of organic solar cells is to cut down the price of process. It can possible to high throughput printing and R2R process. These cells can be processed from the formation of solution. Therefore it is easy to manufacture. The mechanism of OPV is different

from the inorganic semiconductor solar cells, which rely on the large built-in electric field of a PN junction to separate the electrons and holes created when photons are adsorbed. OPV materials have two types, one is the electron door and the other is as an acceptor. When a photon is converted into an electron hole pair, typically in the donor material, the charges tend to remain bound in the form of an exciton, and are separated when the exciton diffuses to the donor-acceptor interface. Short diffusion length for OPV is limits for attaining higher efficiency. Nanostructured inter face, and bulk hetero junction solar cells are proposed for a proper module. Fig 2.4 illustrates the structure of bulk hetero junction solar cells.

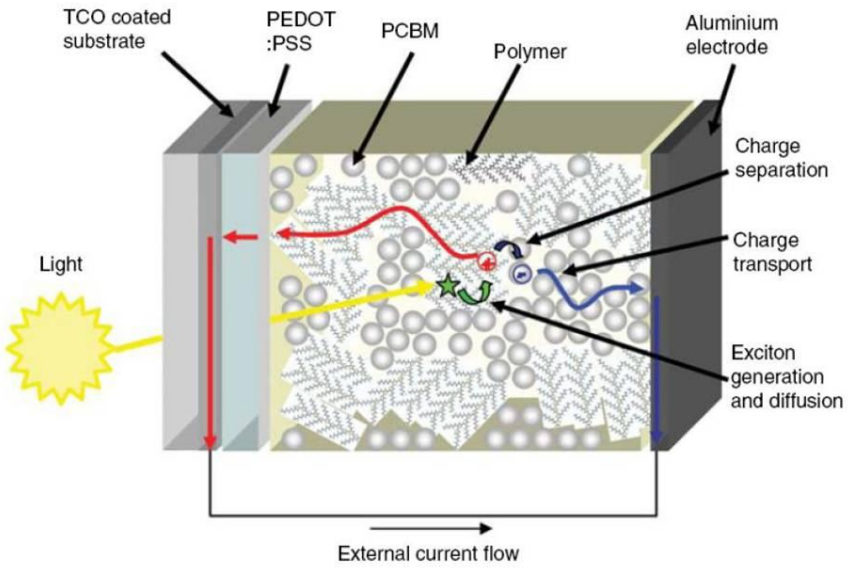


Fig 2.4 The bulk hetero junction type of OPV [24].

Dye sensitized Cells and Quantum dot sensitized solar cells

In the late 1960s, illuminated organic dyes could generate electricity at oxide electrodes in electrochemical cells. Dye-sensitized solar cells was invented by Michael gratzel and Brian O'Regan in 1991. It is based on a semiconductor formed between a photo sensitized anode and electrolyte, a photoelectrochemical system. The below picture is the structure of DSSCs. It is operated at stable performance at nonstandard conditions of temperature, irradiation, and

solar incidence angle. Also, it is available to environmental-friendly raw materials. And it can express semi-transparency and multi-color rage possibilities. However, DSSC has two major problems that have prevented its large scale commercialization. One is the electrolyte. The electrolyte such as iodide limits the device photo voltage 0.7 V. In addition it leads to extremely corrosive, resulting in a lack of durability. The other problem is cathode material. The conventional cathode material is platinum. However the Pt material is expensive, non-transparent and rare.

Compound semiconductor materials (ex QDs) have been applied in this region because of some advantage, such as a tunable band gap, higher exciton coefficient, and large dipole moment. QDs can produce more than one exciton from on high energy photon via multiple exciton generation (MEG). This effect allows one exciton per high energy photon, with high kinetic energy carriers losing their energy as heat [25].

# 3. Theoretical background

## 3.1 Quantum Dots

### 3.1.1 Definition of Quantum Dots

Table 3.11 shows the characteristics Quantum Dots (QDs), which has clusters of 10-50 atoms that have diameters in range of 1-20nm. As particle size becomes smaller than exciton bohr radius, the QDs have quantum confinement effect is regarded. The nanoparticles [26] comes from II/VI, III/VI semiconductor compounds. This unique property become available for the field of optics, luminescence, electronics, catalysis and solar energy conversion.

Table 3.1 Characteristics semiconductors and QDs

| **Properties** | **Semiconductor** | **Quantum Dot** |
|---|---|---|
| **Size** | Bulk material | 2-10nm nano crystalline |
| **Electrons Energy levels** | Quasi continuous | Small band gap is discrete between the valence band and conduction band |
| **Band gap** | Smaller than Quantum Dots | Tune the band bap by the composition, and size |
| **Absorbance** | Uniform absorption spectrum | A series of overlapping peaks |
| **Conversion Efficiency** | 31%<br>Shockley Queisser | Higher than Shockley quisser<br>Multiple exciton generation |

.

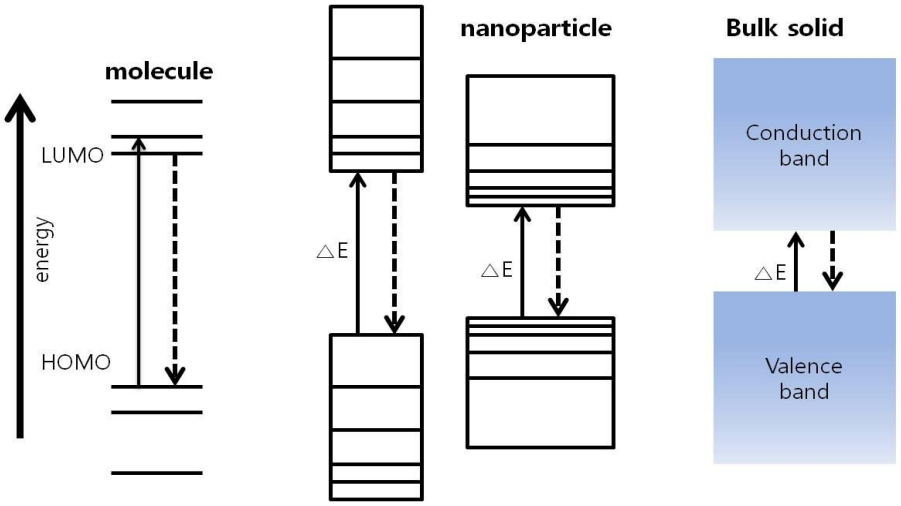


Fig 3.1 Energy diagrams nanoparticles, a molecule and a bulk semiconductor [27].

Quantum confinement effect

Surface atoms have generally a major role in determining free energy and the thermodynamics properties of material. When the size of atom is decreased, the volume of atom surface is increased. Nanoparticles materials have discrete energy value compared to bulk phase due to Pauli exclusions principle. There are no electrons can share the same energy value, it leads to quantum confinement effect. When the quantum dot size is lower than the Exciton Bohr radius, the crowd of electrons induces to split of the original energy levels into smaller ones with smaller gaps between each successive level. Above the Fig3-1 are illustrated. In the case of semiconductor nanoparticles or quantum dots, the DOS (Density of states) shows discrete values.

Particle size

The phenomenon of excitation is defined that the electrons goes up from the valence band to the conduction band after the photon absorption. The electrons in the conduction band will goes down to the valence band when the photon energy have a larger than the band gap. At that time the photon energy is called as the energy of the emitted photon.

This emitted photon energy is determined by the size of the quantum dot due to quantum confinement. The emitted energy of bulk is the sum of the band gap energy. As we discussed before, the DOS of nanoparticles are discrete with decreasing the particle size and will require the higher gap. This formulation expressed. The band gap of nanoparticles is expressed that the relation of the band gap of the bulk state, the confinement energies of hole and the excited electron, and the bound energy of the exciton.

### 3.1.2 The classification of QDs syntheses

The QDs are available for sensitizer in the case of QDSSCs. There are two methods for synthesizing of QDs (In situ, Ex situ)

In situ

QD sensitizers can be directly synthesized by using a method of chemical bath deposition (CBD) or successive ionic layer adsorption and reaction (SILAR). The method of CBD was affected by the composition, time and temperature. All precursors are in the same bath and is grown by ionic reaction

SILAR is simpler than CBD. It can be less controlled by concentration, and time. This process is that semiconductor substrates are dipped into cation solution, washed the substrate, dipped anion solution and washed substrate. Both routes can deposit the higher amount of the sensitizer, but it is hard to control over the size and shapes of QDs.

Ex-situ

QDs are directly attached to the semiconductor without functional group. Pre-synthesized nanoparticles are used. Colloidal nanoparticles synthesis in a suitable solvent medium, which is called as the chemical bottom-up, can obtain nanostructured system. It is possible to get the desired particle size over the largest possible range. The size of colloidal quantum dots is controlled by the reaction time and temperature. In addition to, it has good crystallinity, can

control surface functionalization and have a high luminescence.

The colloidal nanoparticles are attached to the semiconductor via bifunctional molecular groups such as MPA (3-mercaptopropionic acid) and EDT. It has a take advantage of controlling over the size and composition. However, QDs can only adsorbed to the semiconductor surface due to the spatial distance of linker group, regardless of the mesoporous $TiO_2$ structure. This phenomenon can affect the amounts of sensitize are adsorbed to the semiconductor, and electron injection. Generally the efficiency is not much higher than the In-situ.

Colloidal Quantum Dots are traditionally synthesized by chemical process, which compounds are dissolved in the solutions. It is based on precursors, organics surfactants and solvents. The precursor transforms into monomer. If the monomers reach a high enough supersaturation level, the nanocrystal becomes growing. The temperature is the critical factor in determining the nanocrystal growth. It is remained at the high temperature for rearrangement and annealing of atoms during synthesis. And then, it is remained at the low energy level to lead crystal growth. Monomer concentration is also another factor. In case of high monomer concentration, the critical size is relatively small. When smaller particles grow faster than large one, it induces to yield nearly mono-disperse particles. Based on the Ostwald ripening, the reaction called as focuses. This synthesis forms is to be the least toxic of all the different forms.

## 3.2 Quantum Dot Sensitized Solar Cells (QDSSCs)

### 3.2.1 Basic components

QDSSCs were composed of photoanode, electrolyte and counter electrode. The structure of photoanode is that nanoparticles (ex. CdS, CdSe, PbS, and InP) which are used as photo sensitizer are adsorbed on the surface of mesoporous $TiO_2$ film on transparent conducting oxide (TCO) substrates. The polysulfide solution was widely used for the QDSSCs. The counter

electrode has characteristic, which has electrochemical catalytic ability against the redox electrolyte.

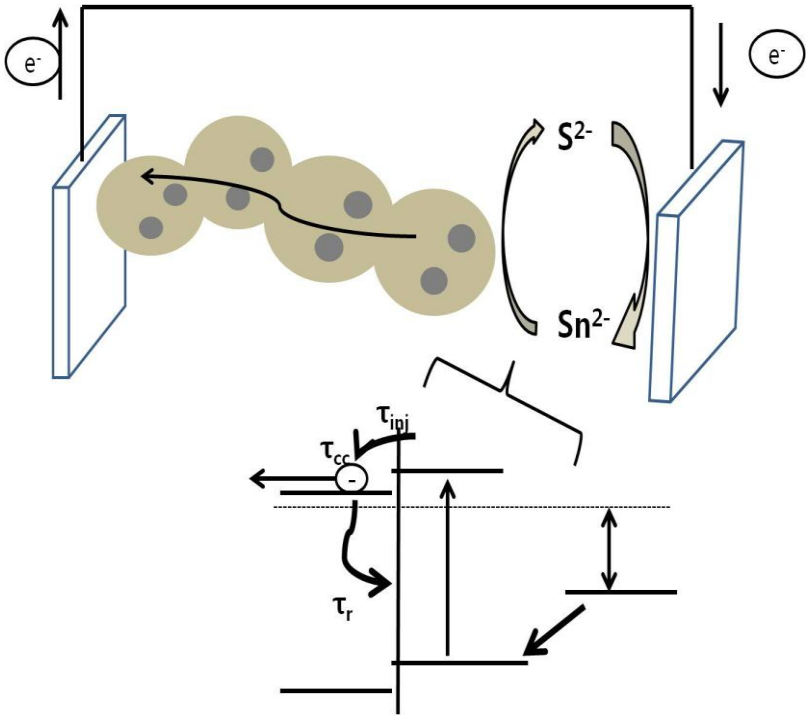


Fig 3.2 Schematic diagram QDSSCs and reaction process.

(1)Transparent counter electrode

The top of cell, bottom of cells are consisted of transparent conducting oxide (TCO) substrates. For the higher efficiency, TCO substrates have low sheets resistance, higher transmittance, and stability. The most widely used substrates is FTO (F-$SnO_2$) substrate, which is more thermally stable than ITO substrate above 450 ˚C. Recently, ITO substrate has been used as flexible substrates. In addition, the both of charge recombination and charge losses are decreased because of affinity between the FTO substrate and $TiO_2$ nanocrystalline materials.

(2) Nanocrystalline metal oxide semiconductor

The widely used photoanode, which has 20 nm nanoparticles, and the thickness is 8-10 μm, is the mesoporous $TiO_2$ electrode for the QDSSCs. Many researchers have been progressed to choose a proper nanocrystalline metal-semiconductor. As the semiconductor has a nanocrystalline surface, it enables a large amount of QD to be adsorbed. However it sometimes leads to the recombination process.

Above all the energy band gap values are considered. The open circuit voltage is controlled the difference between fermi level of semiconductor and the fermi level of electrolyte. Therefore the higher conduction band (CB) of oxide materials is preferred to gain a high circuit voltage. In addition, the conduction band edge of oxide semiconductor is lower than the LUMO level of QD materials for easier migration. $TiO_2$, $SnO_2$, ZnO, $Nb_2O_5$ have been exploited Fig 3.2. As you see Fig 3.3, $TiO_2$ nanocrystalline semiconductor among these semiconductors has been widely known.

$TiO_2$ has three type phases, which are anatase for low temperature, rutile for high temperature, and brookite type. A much larger adsorbed amount of QDs can be adsorbed to the anatase $TiO_2$ film [28] because anatase surface film has much higher surface volume per area. In terms of electron diffusion coefficient, anatase film has much faster the rate of electron transfer.

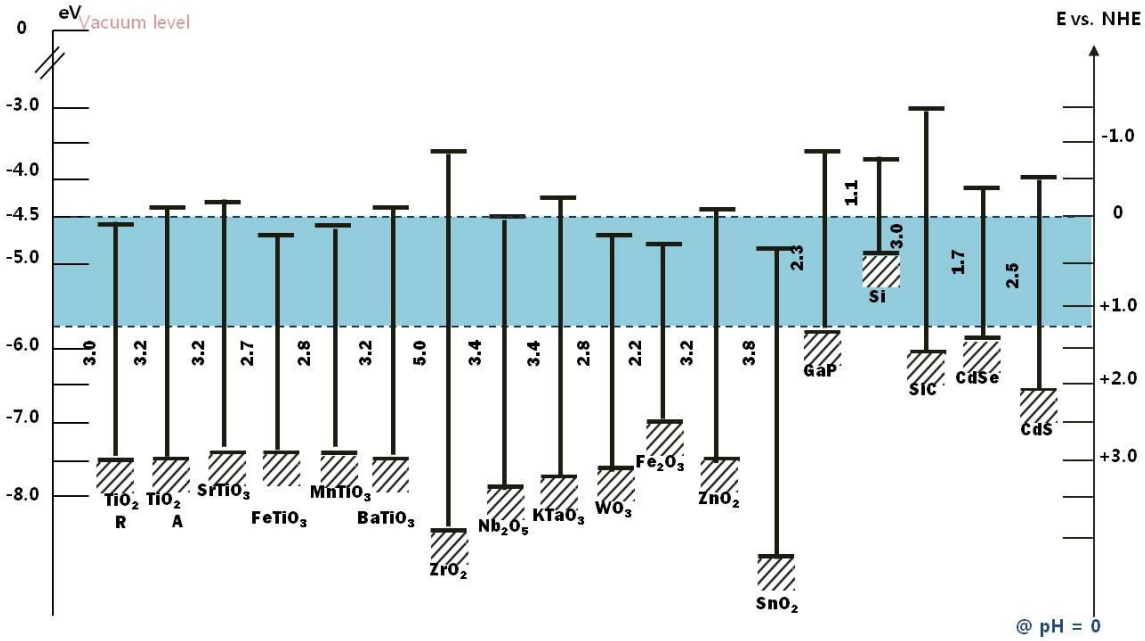


Fig 3.3 Band gap energy of semiconductor

| **Semiconductor** | **$E_{bg}$(eV)** | **$E_{fb}/E_{eb}$ (V) (vs. NHE)** |
|---|---|---|
| $ZrO_2$ | 5.0 | -1.78V (pH 13) |
| $SnO_2$ | 3.5-3.8 | +0.5 (pH 1) -0.1V(pH7) |
| $Nb_2O_5$ | 3.4 | -0.6 V (pH 7) |
| $TiO_2$ rutile | 3.0 | -0.05 (pH2) -0.6V(pH12) |
| $TiO_2$ anatase | 3.2 | -0.28 (pH2) |
| ZnO | 3.0-3.2 | -0.2 (pH1) -0.4V (pH 4.8) |
| WO3 | 2.4-2.8 | +0.3(pH1) -0.15 to +0.05(pH 9) |

Table 3.2 Energy band diagram depending on pH

(3) Redox electrolyte

The most utilized electrolyte for QDSSC is polysulfide electrolyte for the stability. However, the iodide redoxes couple has been used for DSSC. Besides polysulfide solution, the $Fe^{3+}/Fe^{2+}$ and the $Fe(CN)_6^{3-}/Fe(CN)_6^{4-}$ redox systems, both in aqueous solution, have been studied. [29]Recently a cobalt complex redox couple was proposed in [30] Solid-state hole conductors such as spiro-OMeDAT and CuSCN have been used to replace the liquid electrolyte.

(4) Counter electrode

For QDSSCs, Pt counter electrode induces low fill factor and lower efficiency because of charge recombination and Au was alternatively proposed [31] [32].The former research illustrates that metal-chal cogenides such as CoS, $Cu_2S$ and PbS pointed higher electro catalytic activity and longer stability. The most widely used method [33] is that directly exposed the metal foils of Cu, Co and Pb to sulfide solution to obtain an interfacial of metal sulfide. The faced problem is that suffers from continual corrosion and ultimately mechanical instability.

3.2.2 Operating in QDSSCs

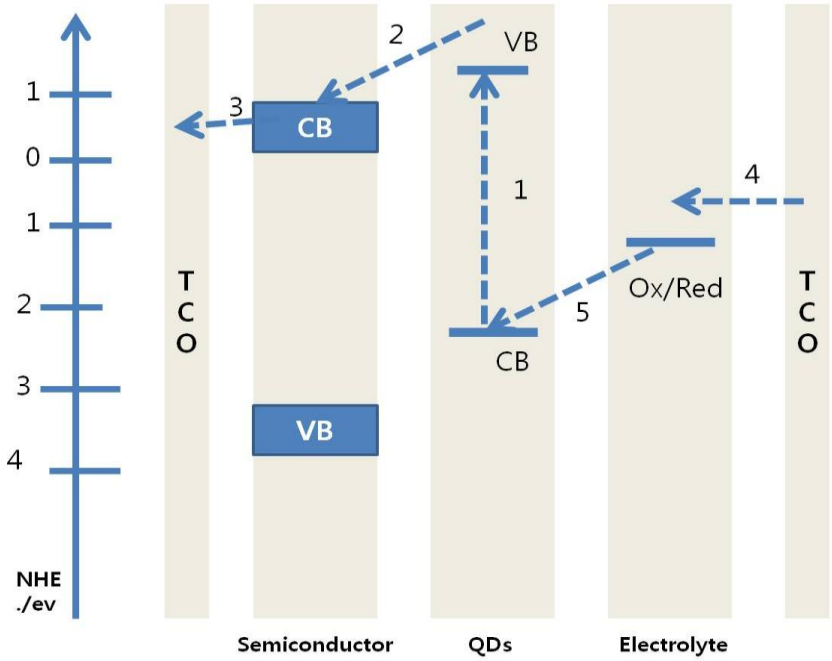


Fig 3.4 Diagram shows electron transfer process shows from photoanode to electrolyte

Above Fig 3.4 shows the process of electrons transfer from the photoanode to electrolyte. QDs go up from the conduction band to the valance band with incident light (1). Then, the exited photoelectrons are rapidly injected to the conduction band of the $TiO_2$ (2). The electrons are transported by the flow through the external circuit (3). The main driving force for electron injection is the gradient in electron concentration. That is, electrons are transported by diffusion. It was believed that most electrons are trapped. Traps generally occur between $TiO_2$ and electrolyte, and at grain boundary. This recombination process [34] involves the transport process, since the both processes take place within milliseconds. The electron transport properties are evaluated by measure the electron life time and diffusion coefficient. The oxidized QDs are regenerated by the redox couple in electrolyte (4) at the counter electrode. The electrons in TiO2 film can be captured by acceptors in the electrolyte (5).

3.3 The performance of QDSSCs

3.3.1 J-V characteristic measurements

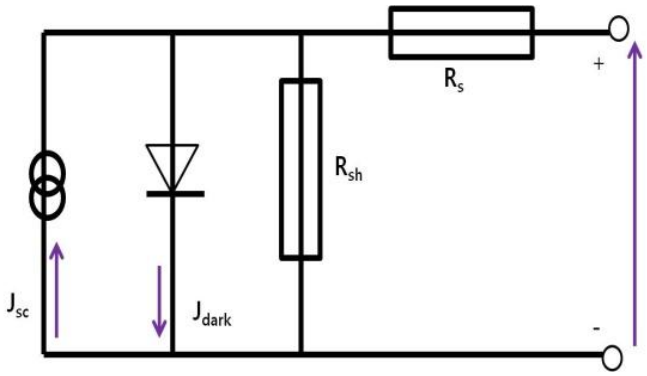


Fig 3.5 J-V curve of solar cells (upper), Schematic circuit of a solar cell (down)

$$\eta = \frac{V_{oc} J_{sc} FF}{P_{in}} \quad \text{- (1)}$$

$$FF = \frac{V_{max} J_{max}}{V_{oc} J_{sc}} \quad \text{- (2)}$$

The photovoltaic power conversion efficiency is determined by above equation (1). Power conversion efficiency (η) is defined that the percentage of photocurrent from adsorbed light, when the electrical circuit is connected All measured values are attained as variable resistance when the light 100 mW $cm^{-2}$ (A.M. 1.5G) is irradiated the side of the photo electrode. Fig 3.5 shows the circuit of photovoltaic cells.

The open circuit voltage ($V_{oc}$) shows applied voltage, a maximum voltage between two electrodes. $V_{oc}$ values correspond to maximum voltage from a solar cell side when the net current is zero through the device. The Voc value for QDSSCs is the difference of energy

band gap between semiconductor and electrolyte.

Short circuit current (Jsc) comes from the amount of electrons with the light, which are generated and collected per the unit cell area. Equation (2) shows that Fill factor (F.F) is the maximum power value divided by the open circuit voltage and the short circuit current.

Resistance is influenced by fill factor, determining power efficiency. $R_{sh,}$ which called as shunt resistance, are generally caused by manufacturing defects. A shunt resistance is particularly considered when light levels are low. Because low light can generate low current. Therefore the loss of electrons has largely affect to the shunt resistance. $R_s$, which called as series resistance, can be attained from the movement of current through the solar cell. It is determined by the resistance of the top and rear metal contacts. To get proper fill factor, shunt resistance should be large to prevent the leakage current and series resistance should be low to get a sharp rise in the forward current.

3.3.2 Incident photon to current efficiency

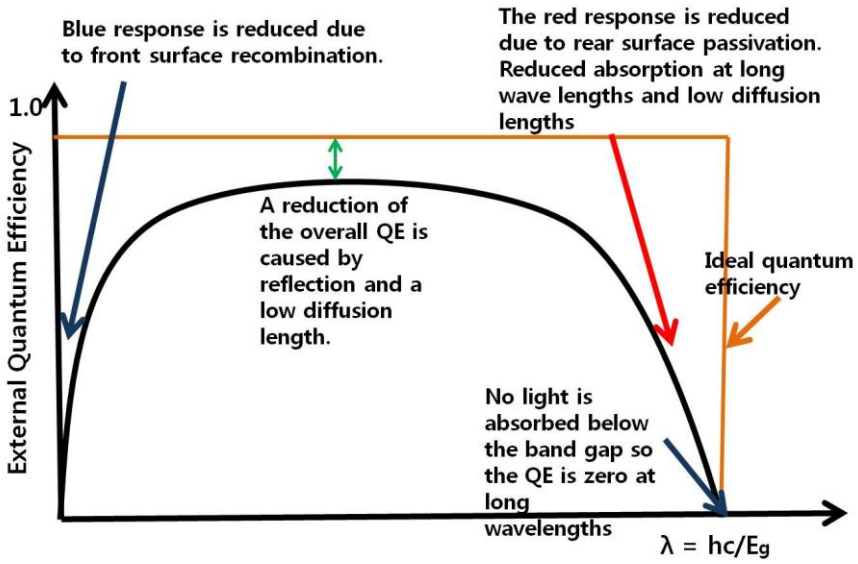


Fig 3.6 Incident photon conversion efficiency graph

As discussed before, one of the main characteristic of quantum dots is the multiple exciton generation (MEG). It means that one photon generate one or two exciton. At that case, we can get over the 100% on the whole spectrum. Quantum efficiency is classified with External quantum efficiency (EQE), and Internal quantum efficiency (IQE).

External Quantum Efficiency is the ratio of the number of charge carriers collected by the solar cell to the number of photons of a given energy shining on the solar cell from outside (Incident photons). It depicts (1). Internal Quantum Efficiency (IQE) is the ratio of the number of charge carriers collected by the solar cell to the number of photons of a given energy that shine on the solar cell from outside and are absorbed by the cell It depicts [35]

$$(1)\quad \mathrm{EQE} = \frac{\text{electrons/sec}}{\text{photns/sec}} = \frac{\text{current/(charge of 1 electron)}}{\text{(total power of photons)/(energy of one photon)}}$$

$$(2)\quad \mathrm{IQE} = \frac{\mathrm{EQE}}{\text{Total Absorption}} = \frac{\mathrm{EQE}}{1-\text{Reflection}-\text{Transmission}}$$

Incident photon to conversion efficiency (IPCE) [36] is classified with the IQE. That means the ratio the number of generated charge carriers by the solar cell to the number of adsorbed photons. It is characterized by the device efficiency over a rage of different wave lengths at each photon energy level.

$$\mathrm{IPCE}\left(\lambda\right) = \mathrm{LHE}\left(\lambda\right)\varphi_{\mathrm{inj}}(\lambda)\eta_{\mathrm{cc}}(\lambda)$$

LHE (λ) is the light efficiency, $\varphi_{\mathrm{inj}}(\lambda)$ the electron injection yield from QD to metal oxide semiconductor, $\eta_{\mathrm{cc}}(\lambda)$ charge collection efficiency at the counter electrode.

# 4. Experimental section

4.1. Synthesis of colloidal QDs

4.1.1 Synthesis of CdSe NCs for sensitizer

Materials

All chemicals were purchased from sigma-Aldrich and used without any further purification.

Precursor

3.21 g of 0.50 M Cd Oxide, 50 mL of Oleic acid were stirred under the vacuum for at least 1 hr. After a change in the $N_2$ atmosphere, the temperature was increased from 100 ˚C to 170 ˚C and kept for 30 min. The solutions were quenched at colorless color.

Selenium 7.90 g was dissolved into 100 mL of TOP into a $N_2$-purged glove box.

The method of CdSe

CdSe nanoparticles were synthesized according to the described method. 1.10 g of TOPO, 1.50 mL of 0.50 M Cd precursor, and 8 ml of 1-Octadence (ODE) were added to a three-neck flask under vacuum pressure at 80 ˚C. A reaction time of 1 hr in the vacuum was needed to dissolve the mixture perfectly. After a change in the $N_2$ atmosphere, the temperature was quickly increased from 80 ˚C to 300 ˚C. At 300 ˚C oleylamine was injected to the three-neck flask and the temperature was decreased to 275˚C. At 300˚C, 4 ml of 1 M TOPSe (selenium dissolved in TOP) was quickly injected and turned off after 3 min. The reaction time caused nanocrystal growth and a color change from clear to yellow to orange was observed. After this hexane and ethanol was added to the solution (hexane:ethanol = 1:3) one time. The liquid

portions were then discarded. Fresh toluene was added to the flocculate. This method was repeated three times to remove unreacted precursors and undesirable synthesis byproducts. The final products were redispersed in the toluene solution.

4.1.2 Synthesis of $Cu_2S$ NCs

$Cu_2S$ were synthesized using Yue Wu, Cyrus Wadia method [37]. All chemicals were purchased from Aldrich and used without any further purification.

1.25 mmol of Ammonium diethyldithiocarbamate in a mixture of 10 mL of dodecanethiol and 17 mL of oleic acid was heated under a vacuum for 30 minutes at room temperature. To prevent oxidation, all chemicals were heated under $N_2$ for 1 hr. and the temperature was swiftly increased from 80 ˚C to 180 ˚C. When temperature reached at 110 ˚C, a solution of prepared copper acetylacetonate (Ⅱ) in 3 ml of oleic acid, was quickly injected to the three-neck flask. Then the solution was quickly heated to 180˚C and the temperature sustained for 20 min. The color of the solution changed in the following order: clear, yellow, red, and black respectively. The $Cu_2S$ NCs was precipitated with hexane and ethanol. This procedure was repeated three times to clean away any residue. The solution was kept in the glove box to avoid any possible oxidation.

4.2 QDs deposition on photo electrode

4.2.1 In-situ [38]

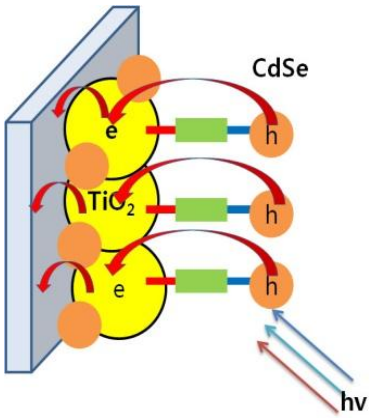


The $TiO_2$ was immersed into HCl solution for 20 minutes. Then, the $TiO_2$ film was washed with D.I water and rinsed with anhydrous acetonitrile. The films were immersed into the 1M MPA (3-mercaptopropionic acid) 0.1M $H_2SO_4$ in anhydrous acetonitrile solution for 12hrs.

Fig 4.1 The structure of photoanode via linker method.

After 24hrs, the films were rinsed with anhydrous acetonitrile and anhydrous toluene. Before the films were immersed into the nanoparticles solution, the nanoparticles were washed with methanol to remove the ligands. The films were immersed into the CdSe NCs solution in anhydrous toluene for 24hrs inside a glove box.

4.2.2 Ex-situ

Successive Ionic layer adsorption and Reaction Process (SILAR) [39]

0.03 M $Cd(NO_3)_2.4H_2O$ was weighed and moved to the glove box. Then, high purity Ethanol was poured and stirred/purged for 1hr to make a metal nitrate solution. 30mM $SeO_2$ was placed into vial with rubber cap under $N_2$ atmosphere for 1-2 minutes and 60mM $NaBH_4$ was added to the vial. Then the reduction process was confirmed by color changes after the 60mM $NaBH_4$ was added. At first, the color was pink, then changed to red and finally dark red. The process of reduction was finally complete when the solution changed to white. It took about 1hr. The final product was moved into the glove-box.

The photoanode was made inside a glove box for stability. The $TiO_2$ electrode was immersed into the $Cd^{2+}$ solution for 1min and was dipped into a $Se^{2-}$ solution successively for 1min. The two step immersion was considered as one-cycle. For each photoanode cell, the

process was repeated at least 7times. As increasing the repeat number of solution, CdSe nanoparticles are increasing. Fig 4.2 (b) shows the color change of photoanode with the number of immersion. A longer washing time with ethanol was needed to remove excess precursors using a pure ethanol solution and the electrodes needed to be dried.

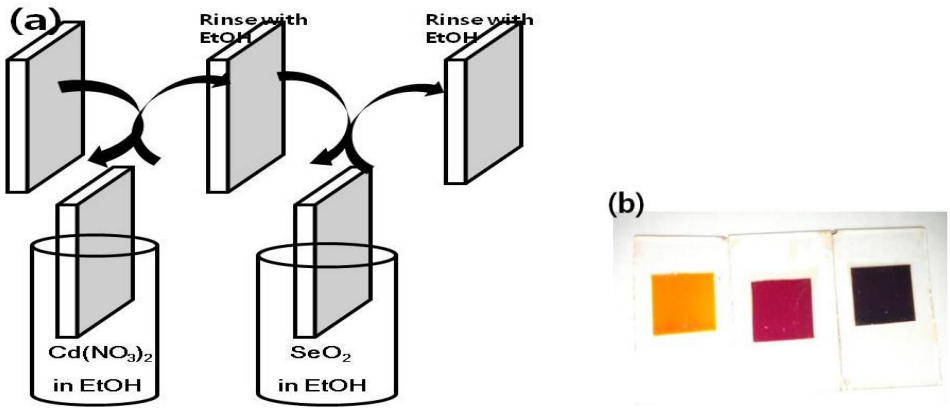


Fig 4.2 (a) The illustration of SILAR method (b) The photographs of the photoanode color after SILAR deposition of CdSe. Yellow color (3 cycles), Red color (5 cycles), and Dark red color (7 cycles)

4.3 Fabrication and assembly of QDSCs

4.3.1 Fabrication of $TiO_2$ photo electrode.

To prepare the mesoporous $TiO_2$ film, the transparent conductive oxide FTO (F-doped $SnO_2$) was completely cleaned. Dust on the FTO substrates were cleaned with soap and water, acetone, methanol, and IPA (isopropyl-alcohol) under sonication for 30mins each. The compact $TiO_2$ layer was deposited by doctor blade $TiO_2$ paste (Ti-Nanoxide T/SP, solaronix) on to FTO substrates, by sintering at 450 ˚C for 30 min. The cross sectional image resulted that the thickness of $TiO_2$ was about 8.17 μm. The thickness of porous $TiO_2$ was controlled by adhesive tape. The cells' active area was 0.24 $cm^2$ for Ex-situ method. And the cells active area was 0.09 $cm^2$ for SILAR method.

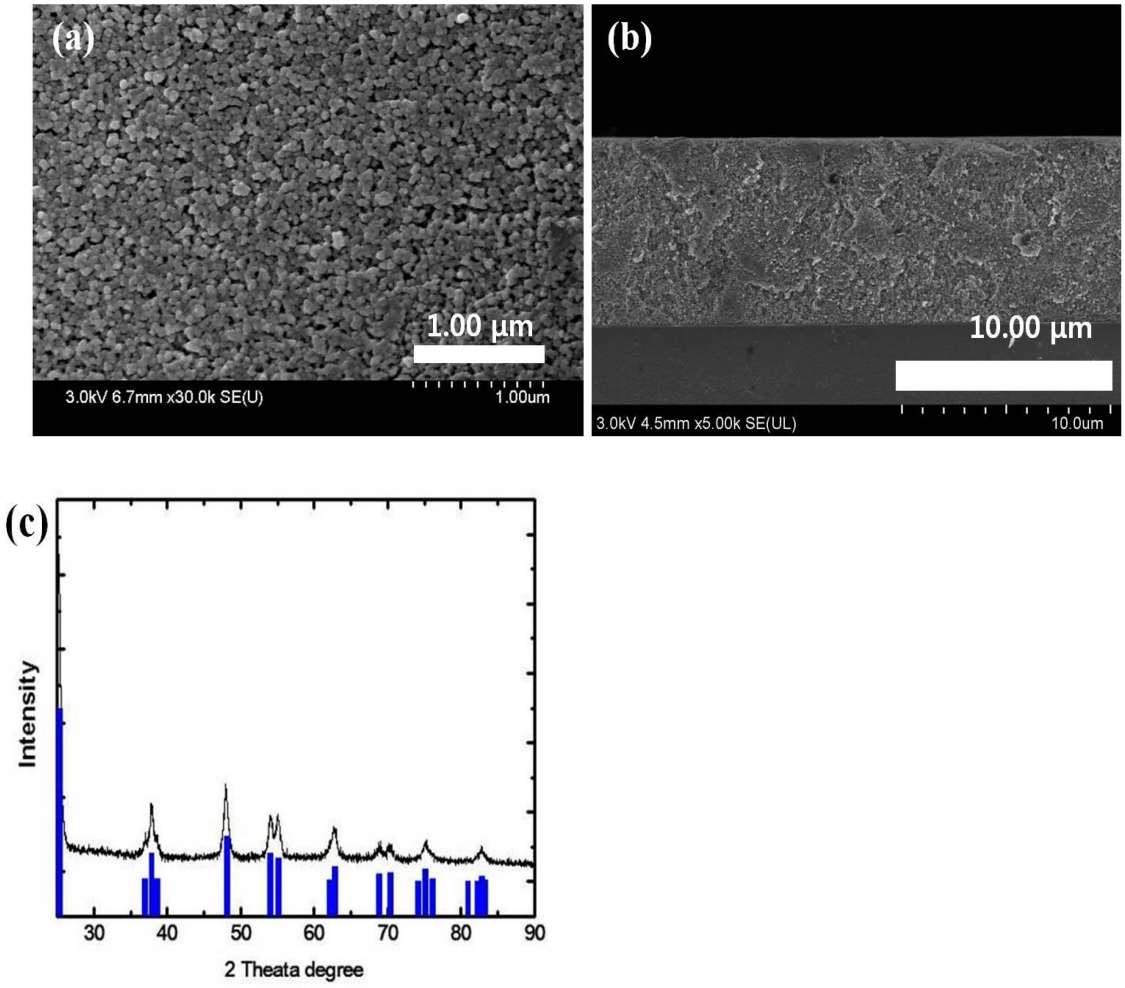


Fig 4.3 (a) FE-SEM surface image of bare $TiO_2$ films. Particle size is about c.a. 20 nm. (b) The width of cross sectional is 8.6 μm. (c) The XRD diffraction pattern of $TiO_2$, which can be confirmed to anatase $TiO_2$ nanocrystals (ICSD 01-086-1157)

4.3.2 Fabrication of counter electrode

The method of making organic counter electrode

After the final products were precipitated, NCs were redispersed by the magic solution (hexane:ocatane = 9:1). The NCs were dispersed onto the FTO via a drop casting. After making the counter electrode, it is need to be sintered at 110 ˚C for one hour to evaporate the organic solvent in glove box.


Fig 4.4 The illustration of making counter electrode

The formation organic capped $Cu_2S$ to inorganic capped $Cu_2S$ [22]

All process was done under the nitrogen atmosphere. Below 0.25 mol of $Na_2S$ (Inorganic ligands) were prepared into formamide. Colloidal $Cu_2S$ NCs with organic ligands were prepared into Hexane. For ligands exchange, 300 μL of $Na_2S$ ligands in 1 mL of formamide were mixed with 300 μL of $Cu_2S$ NCs in hexane. The solution of foramide was not immiscible with hexane. The mixture was stirred for 10 minutes to complete the ligands exchange. The phase transfer can be checked, confirming hexane phase. Color was changed from black to colorless. The top hexane part was poured and $Na_2S$ of inorganic parts were be done by washing three times to remove any remaining hexane part using hexane solution. At that time, excess of toluene was poured to that solvent. And then the acetronitrile (Solution:Acteronitrile = 1:0.75) was added to precipitate the colloidal $Cu_2S$ NCs. Isolated $Cu_2S$ NCs were redispersed by Dimethylsulfoxide (DMSO).

The surface of NCs have long hydrocarbon chain by traditional colloidal method, which introduce insulating layer around each NCs. Talaphin group reported [22] that to replace inorganic (metal chalcogenides) ligands preserve optical adsorption properties. Also, Electron mobility markedly had been enhanced. The role of Halide anions will enhance electronic transport.

4.3.3 Assembly of QDSSCs

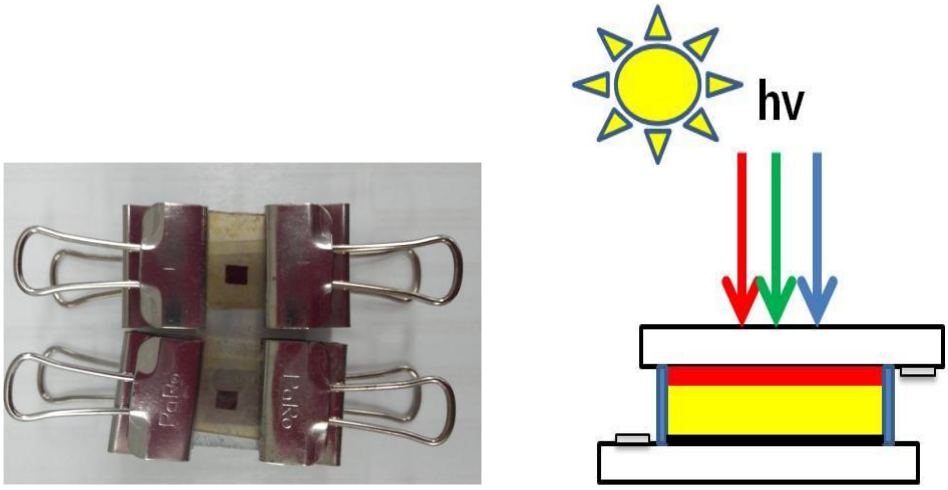


Fig 4.5 Configuration of sandwiched cell employed in photoelectrochemical measurements. Yellow=Polysulfide electrolyte; Black=$Cu_2S$ NCs counter electrode; Red=quantum dot sensitized $TiO_2$; Blue=Surlyn polymer spacer; Black outline with white fill=FTO conductive glass substrate; Grey=connection parts (left).
The picture of real cell (Right).

The electrolytes were used 2 M sulfur, 2 M sodium sulfide and 0.2 M potassium chloride in methanol:water (=7:3). The compact cells were assembled with sealant (SX 1170-60, Solaronix). The liquid electrolytes were injected into the cell to measure a photoelectrochemical measurement.

# 5. Result and Discussions.

## 5.1 Characterization of QDs and QDSSCs

### Materials characterization

The CdSe, $Cu_2S$ nanocrystals absorption spectra were recorded by Agilent cary-5000 UV-Vis-NIR. 30 μL NCs solution was added to the solution solvent to measure the absorption. CdSe photoluminescence was characterized by Agilent Fluorescence spectroscopy. A HITACH S-4800 SEM was used to investigate the surface morphologies and cross sectional image of photoanode and counter electrode, respectively. This SEM images were attained at 3 kV with a working distance of 13mm directly on conductive FTO substrates. The surface of photoanode via In-situ was checked by Energy dispersive spectroscopy. The shape and size of nanoparticles were characterized by FE-TEM 3300/NB5000/S-4800. TEM copper grid was used to characterize QDs. XRD diffraction pattern were measured by Pananlytical empyrean. And then XRD data were obtained by placing the materials directly are placed on the glass under X-ray beam while the detector angle was scanned from 25° to 90°.

### Electrochemical and photo electrochemical characterization

The current density- voltage (J-V) measurements of devices were performed using a McScience Inc. K-3300 under 100 mW $cm^2$ AM 1.5 G illuminations. All measurements were carried out under ambient conditions at room temperature. The active area of the cells 0.09$cm^2$ and 0.25$cm^2$

Electrochemical impedance spectroscopy (EIS) data was measured at the frequency range from 0.005 kHZ to 1000 kHZ at room temperature. OCV, CV graph were performed at a scan rate of 10 $mVs^{-1}$.

5.1.1 Optical characterization of QDs

The UV-Vis-NIR absorption spectrum of the pre-sensitized CdSe QDs (Fig 5-1 (a)) in toluene solution exhibits a lowest energy peak at 541nm (~2.36 eV) [40] [41].

$$E_{QD} = E_g + \frac{h^2}{8r^2}\left[\frac{1}{m_e^*} + \frac{1}{m_h^*}\right] - \frac{1.8e^2}{4\pi\varepsilon\varepsilon_0 r}$$

$E_{QD}$ the lowest excitation energy of the QDs, Eg the band gap of bulk, r is the radius of QDs particle, $\varepsilon_0$ vacuum permittivity, ε relative permittivity, $m_e$ and $m_h$ is the effective mass of electron and holes, respectively. According to the Brus equation above, the diameter particle size is expected to 2.8nm. The band gap of bulk CdSe is 1.65eV[42].

Fig 5.1 (b) shows the size of CdSe NCs with TOPO ligands shows 2.8nm by a TEM image, which is in accordance with absorption spectra. The particle energy level relative to the vacuum is based on the particle diameter. The particle CB energy level is calculated ~2.3eV *vs Vacuum* as the borreli. Mesoporous $TiO_2$ electrode energy level is ~3.2eV *vs Vacuum*. Therefore the QDs are easily injected from the QDs to the $TiO_2$ electrode. Therefore QDs are easily injected into the $TiO_2$ semiconductor because the CB level of the QD is higher than the conduction level of $TiO_2$ semiconductor. Fig 5.2 illustrates the band diagram of this cell's configuration using colloidal nanoparticles. In case of SILAR, the CdSe particle size (7 cycles) estimates the 4.5-4.9nm. As increasing the number of immersion, the peak will be shift to red. We estimate the optical band gap of QDs by intersecting the base line and the shoulder line. Therefore it is easily transfer to the semiconductor compared to colloidal NPs method.

The metal sulfide has been attracted due to the Pt expensive cost and the poisoning effect. The method, which is foil exposed to a sulfide solution, has been used until now to obtain the metal sulfide interfacial layer. The process is easy; however it leads to instability and continual corrosion. We propose counter electrodes using nanoparticles due to higher surface, mass production. In the result, we can get higher performance when copper sulfide counter electrodes are used compared to Pt electrode. It turns out that nanoparticles have distinct surface charges. Therefore it induces to the facile deposition on the electrode via electrostatic self assembly. We synthesize colloidal $Cu_2S$ NCs, which is processed with the reaction between copper (II) actylacetonate and ammonium diethyldithiocarbamate in mixed solvent of dodecane thiol and oleic acid. The optical property of $Cu_2S$ NCs (Fig 5.3 (a)) shows a wide absorption of up to approximately 1000nm. $Cu_2S$ NCs has been confirmed by XRD diffraction pattern, TEM image. Fig 5.3 (b) shows that the synthesized solution have hexagonal chalcocite (ISCD 00-046-1195) structure. The TEM image (Fig 5-3 (c)) confirms the size of $Cu_2S$, which is c.a. 4-5nm. The metals sulfides NCs were dispersed onto the FTO via drop casting in the nitrogen atmosphere to avoid any possible oxidation. The major role of counter electrode is that has attained a higher electrical catalytic activity. The monolayer formation on the FTO via drop casting is preferred for attaining higher efficiency solar cells. The self assembly method is used to higher surface coverage. After precipitating pre synthesized colloidal nanoparticle, the supernatant is discarded. A magic solution (hexane: octane=9:1) is added to be redispersed. And then the particles get have charges. That solvent induces self assembly onto the substrate. Fig 5.4 is the images of cross sectional (a) and surface morphology (b) via drop-casting. After depositing the solution on the FTO, the film is annealed at 130℃ for 1 hrs. The film was annealed to crystallize the $Cu_2S$ NCs solution and dry the organic solvent. All process did under the nitrogen atmosphere to avoid possible oxidation.

5.1.2 Characterization of photovoltaic performance of QDSCs

There are two methods to attach CdSe QDs to the $TiO_2$; colloidal nanoparticles method and SILAR method.

Colloidal quantum dot adsorption onto the semiconductor involves many factors (QD concentration in immersed solution, QDs particle size, surface and solution clearness, surface treatments), which is difficult to control. Therefore the immersion time is longer to reduce the other factors effect. In addition, the particle size particularly considered due to nanocrystalline structure. The average QD's size are smaller, the large amount of QDs is adsorbed onto the semiconductor.

Fig 5.6(b) shows the FE-SEM surface morphology image to attach the colloidal CdSe NCs to the $TiO_2$. The $TiO_2$ film was preferentially immersed in the acetronitrile solution, which has bifunctional group, to have a negative charge. In case, we here investigate two factors; the particle size and ligands around QDs affect to attach the QDs to the semiconductor of the $TiO_2$. The $TiO_2$ semiconductor has mesoporous structure; therefore QDs with the smaller size can be easily adsorbed. At the optimized condition, the size of colloidal CdSe NCs is 2.8nm. The CB level of QDs does not match with the conduction band of the $TiO_2$ with above 2.8nm particle size. After synthesizing material, there remain excess reaction precursors and undesirable byproducts on to the QD surfaces. QDs particles are washed at three times to washed away the excess precursor, and byproduct. Synthesized CdSe particles around have TOPO ligands, it has neutral charge at first time. It leads to increase the average polarity because TOPO ligands are eliminated. As eliminating TOPO ligands, particles become larger. In that, they have larger van der waals forces, which cause stronger interaction between QDs and semiconductor film with MPA. Therefore it can be improved the QD affinity toward semiconductors. The number of washing times should be monitored closely. We are careful of washing process because instability and aggregation occurs from too much washing times. Fig 5.5 shows the UV_Vis_NIR curve with increasing the number. There is little peak change,

which means there is no size change effect. These results showed higher correlation between washing process and high adsorption for efficient photovoltaic conversion efficiency.

Fig 5.7 a, b shows the morphology image of film that QDs were deposited on the semiconductor via the in-situ method. $TiO_2$ film is immersed cation solution & anion solution alternatively. It is difficult to control the size of QDs and morphology. As increasing the number of cycle, the size of QDs is increased. At that time, QDs were not exactly the spherical form, was deposited forming anion and cation layer by layer. Fig 5-7 (a) image shows the QDs are deposited with 3 cycles. Fig 5.7 (b) image QDs are deposited with 5 cycles. The CdSe QD's size and coverage increases with increasing the cycle number. The energy dispersive X-ray spectroscopy (EDS) (Fig 5.7 (c) and (d)) shows the photoanode are successfully deposited.

5.2 The effects of counter electrodes on the QDSSCs performance.

The J_V graph shows the photoelectrochemical power conversion efficiency, as different method of making photoanode and different counter electrodes under regenerative polysulfide (2 M $Na_2S$/ 2 M S) redox couple. All photoelectrochemical measurements were done under AM 1.5G, $100mW^{-2}$. We adopt below values, which were the open circuit voltage ($V_{oc}$), short circuit current ($J_{sc}$), Fill factor (F.F) Efficiency ($\eta$), to evaluate the performance solar cell. The cell's area was 0.09 $cm^2$ in case of SILAR method with Pt, $Cu_2S$ NCs counter electrode. And the other's cell area was 0.24 $cm^{2.}$ Table 3 shows the performance results as various counter electrode when the photoanode is same. Also, it can show the results as the different method of making photoanode.

The short circuit current ($J_{sc}$) 5.99 $mA/cm^2$, the open circuit voltage ($V_{oc}$) 0.31V with the $Cu_2S$ NCs counter electrode via in-situ method was attained. We confirmed that the short circuit current, the open circuit voltage was slightly higher compare with Pt counter electrode. This materials has a large production limit, and expensive cost when Pt paste was used as

counter electrode. In substitute for Pt, $Cu_2S$ NCs counter electrode has been proposed properly. The Cu2S counter electrode is higher efficiency, higher fill factor than Pt electrode. Fig 5.4 illustrates electron hole pairs occur at the photoanode. In case of charge separation, electron goes through circuit and hole forward to the electrolyte. Significantly impaired charge transfer occurs when Pt is used in the conjunction with polysulfide. Therefore polarization resistance and over potential is high. That's why the cell performance is decreased. However when $Cu_2S$ is connected as counter electrode, it is easily transfer.

According to the reference data, we synthesize 2.7 nm colloidal QDs and adsorbed mesoporous electrode. Being assumed the solution concentration 0.08 mM same that is made by me, we immersed the semiconductor film in the QD solution for 24 hrs to obtain high QDs loadings. Fig 5.9 shows Voc, Jsc, F.F, efficiency with a colloidal nanoparticle method. This data shows the efficiency is relatively low although the advantages that control the size and morphology. Jsc is decreased due to the presence of linker group. The role of bifunctional group reduces electron tunneling injection by separation between QDs and electrode materials. As discussed before, the adsorbed amount of sensitizer (Fig 5.6 (a)) are related to efficiency.

The electrical catalytic activity demonstrated $Na_2S$ capped_$Cu_2S$ NCs has much higher performance than Organic capped $Cu_2S$ NCs. However, Fig 5.10 J-V result seems that there are no difference, these results comes from when the charge recombination occurs between photoanode and electrolyte.

We did solar cell performance test with using other type of counter electrode and using other method that makes photoanode to get higher efficiency and fill factor, we can't get above 1%. The proper band gap alignment is considered to optimize this condition. Whereas Conduction band of CdSe is above $TiO_2$ semiconductor; it was not perfectly match to inject semiconductor.

5.3 The study of electrochemical characterization

The objective of electrochemical study is to illustrate the relation between ligands exchange and the rate of redox reaction. It expects that the efficiency will be increased when the photoanode combines with $Na_2S$ capped $Cu_2S$ NCs counter electrode due to fast charge transfer.

We carried out EIS (Electrical impedance spectroscopy), LSV (Linear sweep voltammetry), and CV(Cyclic voltammetry) measurements to investigate the interfacial layer phenomenon between the polysulfide solution and counter electrode using three electrode cell, which consists of a working electrode, Pt as counter electrode, SCE used as reference electrode. LSV is focused on the redox reaction($Sn^{2-}+e^{-}\rightarrow nS^{2-}$) between the counter electrode and electrolyte. The organic capped counter electrode and $Na_2S$ capped counter electrode used as the working electrode. Three electrode cells are immersed into the polysulfide solution.

Fig 5.11 (a), (C) shows the CV, LSV data of 2M/2M $Na_2S$/S using $Na_2S$ capped $Cu_2S$ NCs working electrode yield currents that are three times greater than observed with an organic capped counter electrode. It means that $Na_2S$ capped $Cu_2S$ counter electrodes have a higher electrical catalytic activity compared to organic capped counter electrode.

EIS data (Fig 5.11 (b)) involves electrochemical internal resistance, and the adhesion between the counter electrode and electrolyte. Smaller internal resistance shows that the catalytic material is more strongly attached to FTO substrates. As you see the data, $Na_2S$ capped NCs have higher internal resistance. It means that the $Na_2S$ counter electrode is not unstable and the adhesion is not strong enough on FTO. Organic capped NCs counter electrodes have much higher charge transfer resistance. This result is in accordance with CV, LSV graph. In

the conclusion, $Na_2S$ capped $Cu_2S$ NCs induces faster charge transfers, whereas the solar cell efficiency is almost the same as organic capped NCs counter electrode.

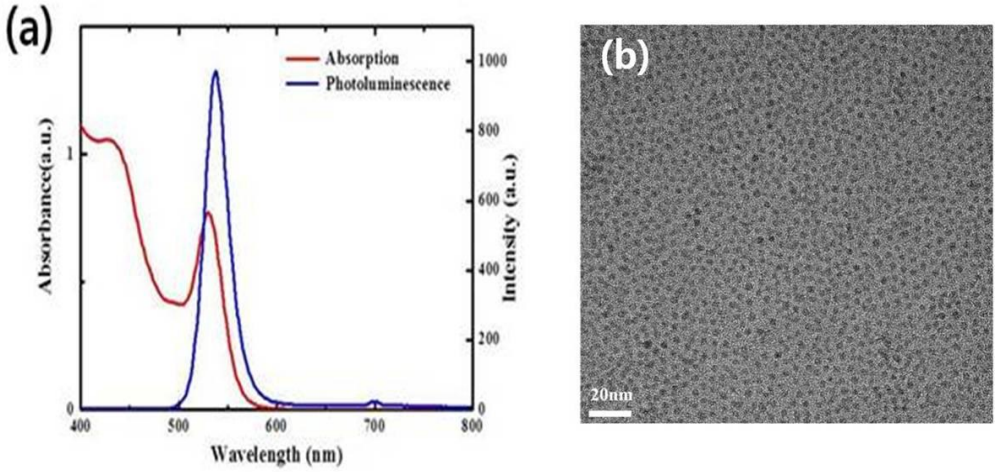


Fig 5.1 Properties of CdSe $NC_s$. (a) UV_Vis_NIR absorption and Photo Luminescence (PL) spectrum of CdSe $NC_s$ in Toluene. Excitation peaks at 541 nm, and emission spectra is showed a little red shift. Then PL peak at 550 nm. (b) TEM image of CdSe NCs with an average diameter of c.a. 2.5-3 nm.

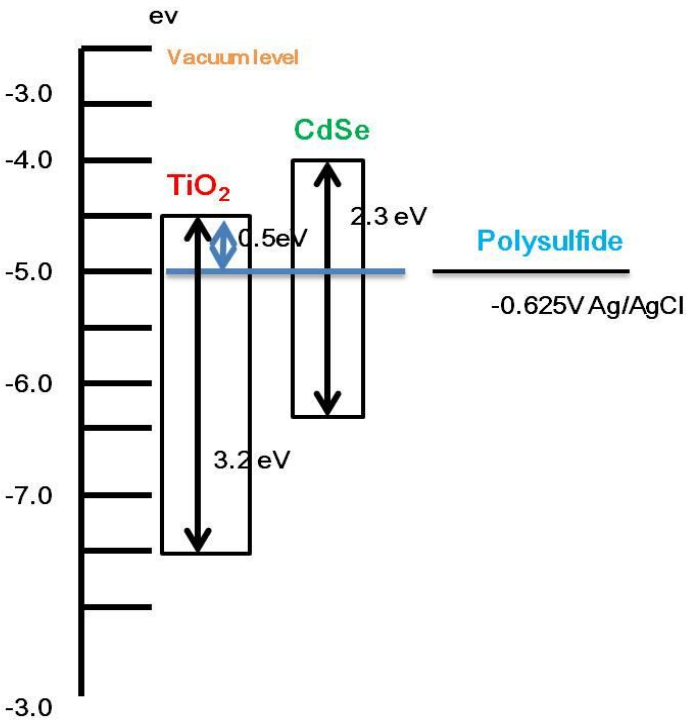


Fig 5.2 Band diagram shows the main energy levels which is involved in charge transfer from semiconductor to polysulfide.

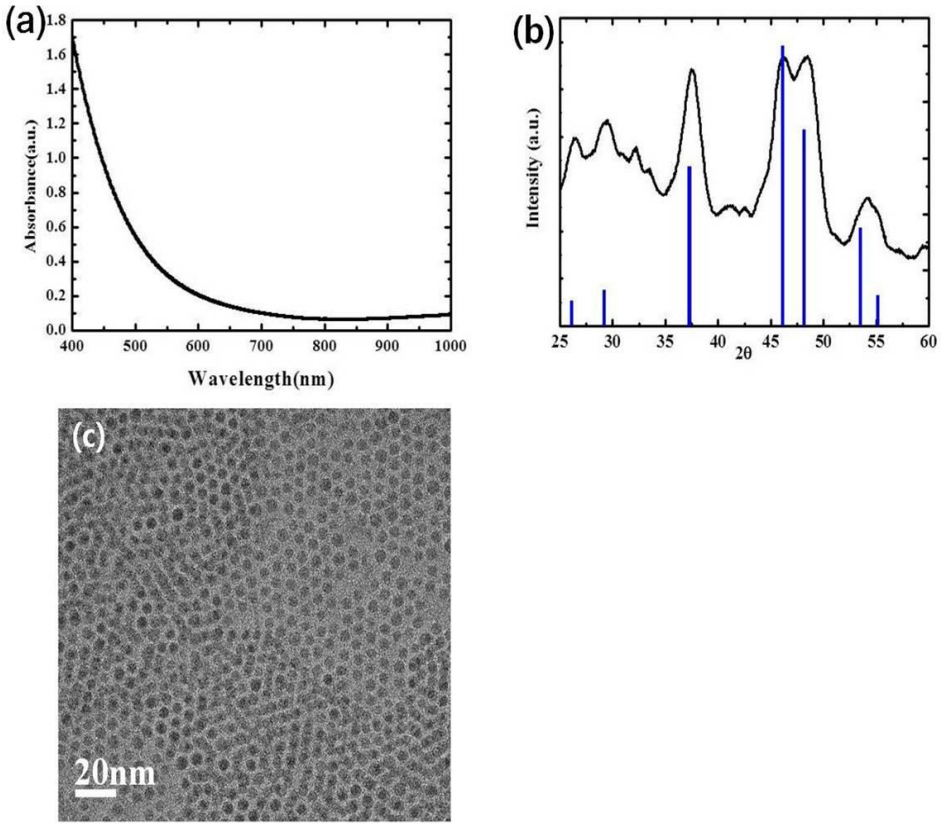

Fig 5.3 Optical characterization of $Cu_2S$ $NC_S$. (a) UV_Vis_NIR absorption of $Cu_2S$ NCs shows a wide absorption up to c.a 1000nm. (b) XRD diffraction pattern of $Cu_2S$ NCs (ICSD 00-046-1195) (c) TEM image of $Cu_2S$ $NC_S$ with an average diameter of ca. 4-5nm.

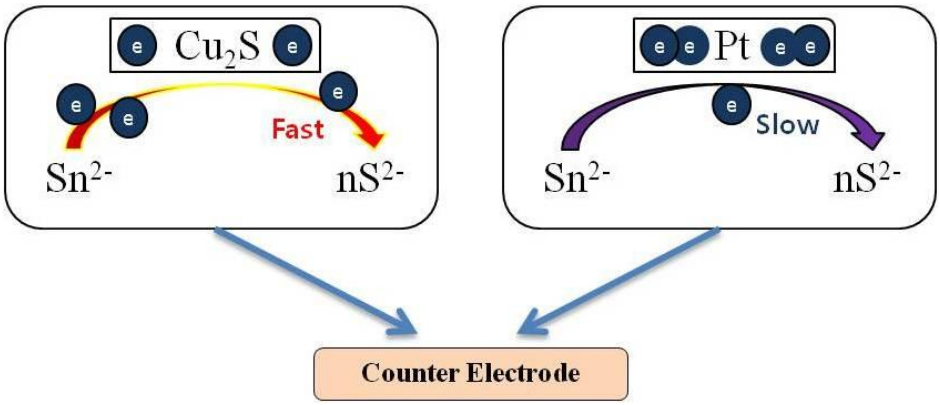


Fig 5.4 Charge transfer easily occurs from photoanode to counter electrode.

Easily charge transfer occurs when $Cu_2S$ counter electrode is used in conjunction with polysulfide electrolyte.

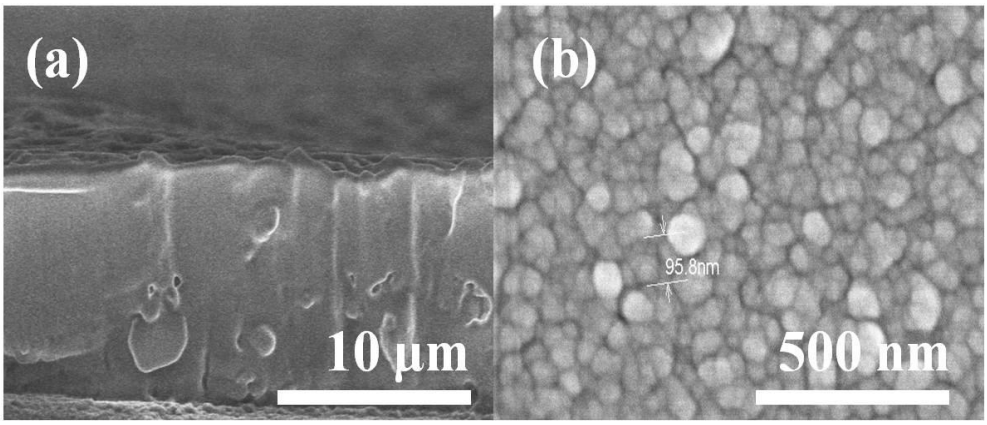


Fig 5.5 The SEM images of $Cu_2S$ $NC_S$ surface (a) Cross sectional image and width 9.6µm (b) The surface morphology of $Cu_2S$ $NC_S$

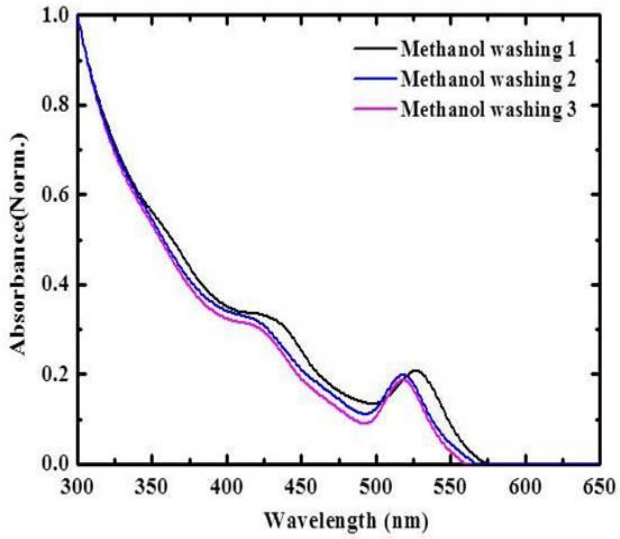


Fig 5.6 UV_Vis_NIR curves of colloidal CdSe $NC_S$ as increasing the number of washing process.

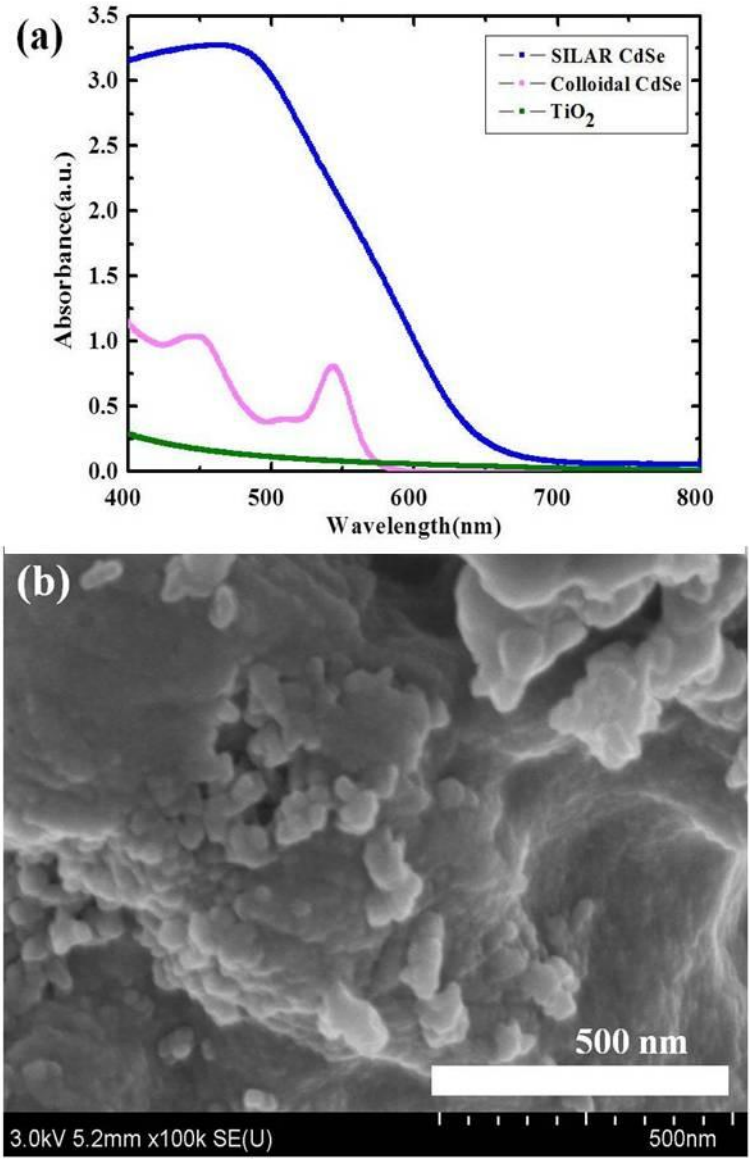


Fig 5.7 (a) Absorbance curves of the bare mesoporous $TiO_2$ film, CdSe film with Colloidal nanoparticles method, CdSe film with SILAR method (b) The SEM morphology CdSe deposited on to the $TiO_2$ film using a linker method

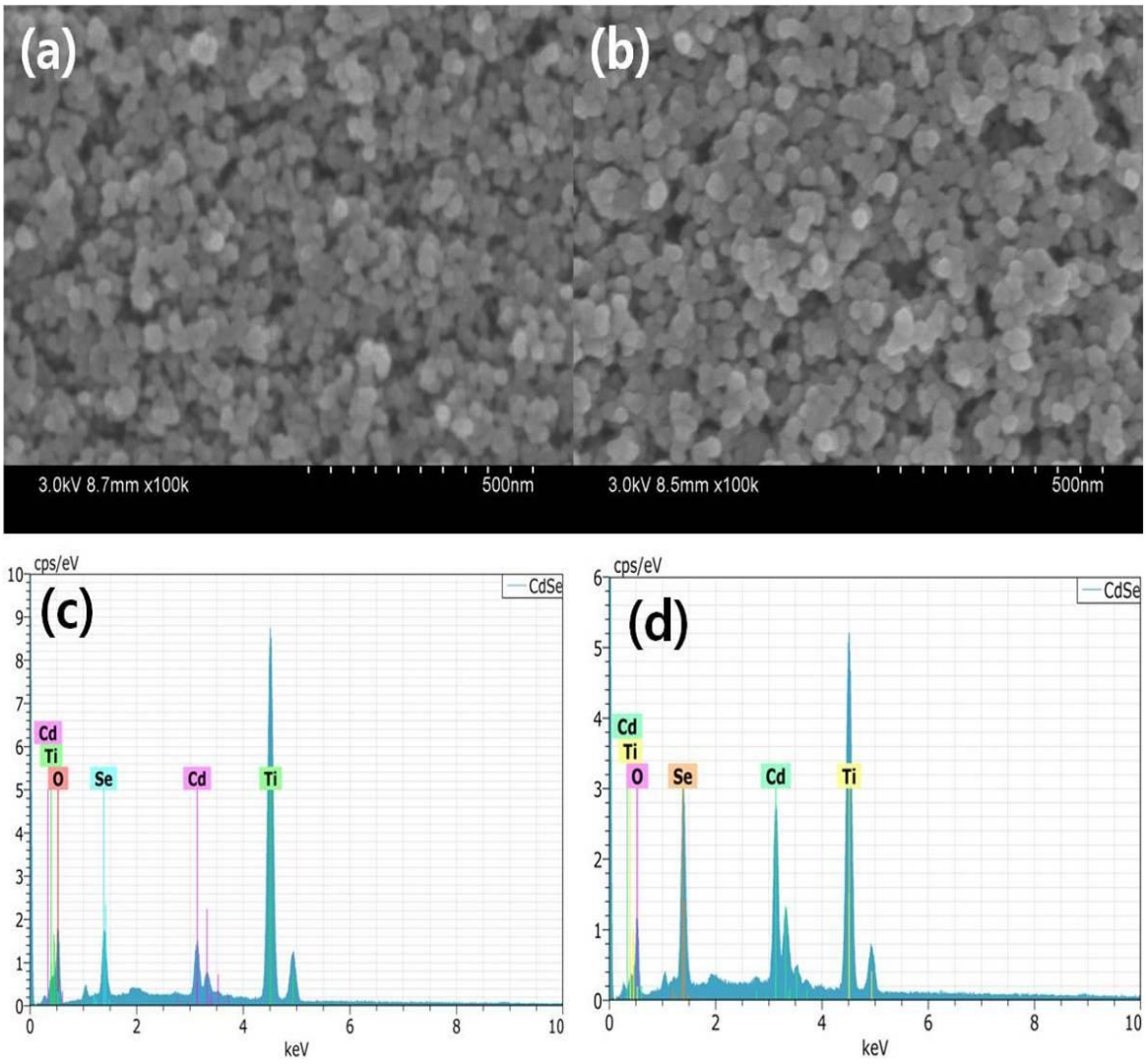


Fig 5.8 FE-SEM surface images according to SILAR cycles. (a) CdSe QD deposited 5 cycles. (b) CdSe QDs are deposited 7 cycles. (c) EDS spectrum with CdSe QDs 5 cycles. (d) EDS spectrum with CdSe QDs 7 cycles.

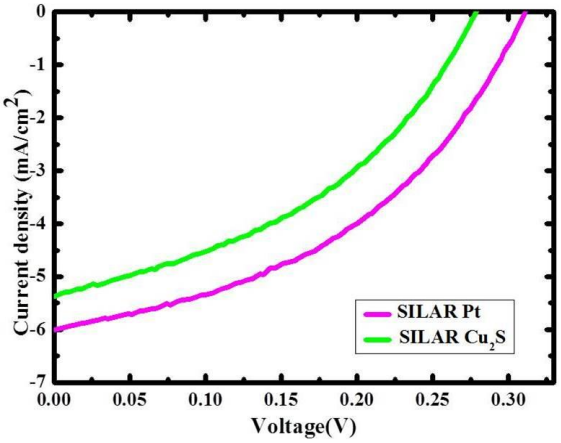


Fig 5.9 J-V curves are compared Pt counter electrode with $Cu_2S$ counter electrode.

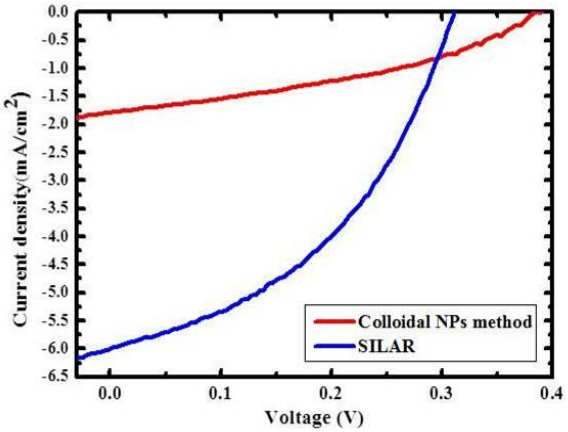


Fig 5.10 J-V curves of QDSSCs depending on the method of making photoanode.

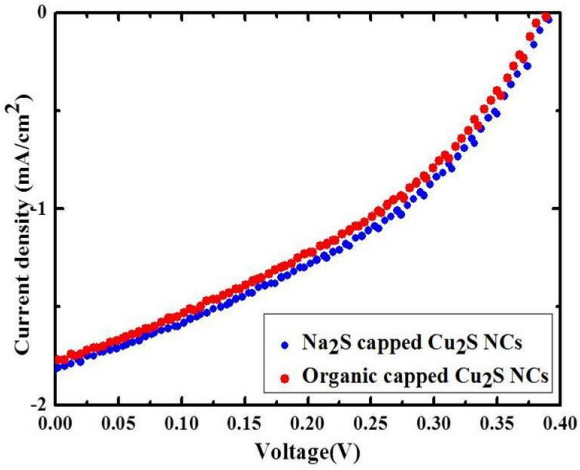


Fig 5.11 J-V curves of QDSSCs depending on the $Cu_2S$ counter electrode using ligands exchange.

Table 5.1 Photovoltaic performance of the QDSSCs measured 1 sun illumination.

| | Samples | Voc / V | $J_{sc}$ / $mAcm^2$ | FF | η(%) |
|---|---|---|---|---|---|
| **Counter electrode Effect** | **SILAR_Pt** | **0.27** | **5.37** | **0.38** | **0.61** |
| | **SILAR_Cu2S** | **0.31** | **5.99** | **0.40** | **0.8** |
| **Photoanode** | **SILAR** | **0.31** | **5.99** | **0.42** | **0.8** |
| | **Colloidal NPs method** | **0.38** | **1.77** | **0.38** | **0.38** |
| **Ligands Exchange** | **Organic_ capped $Cu_2S$ NCs** | **0.38** | **1.77** | **0.37** | **0.27** |
| | **$Na_2S$_capped $Cu_2S$ NCs** | **0.38** | **1.81** | **0.38** | **0.28** |

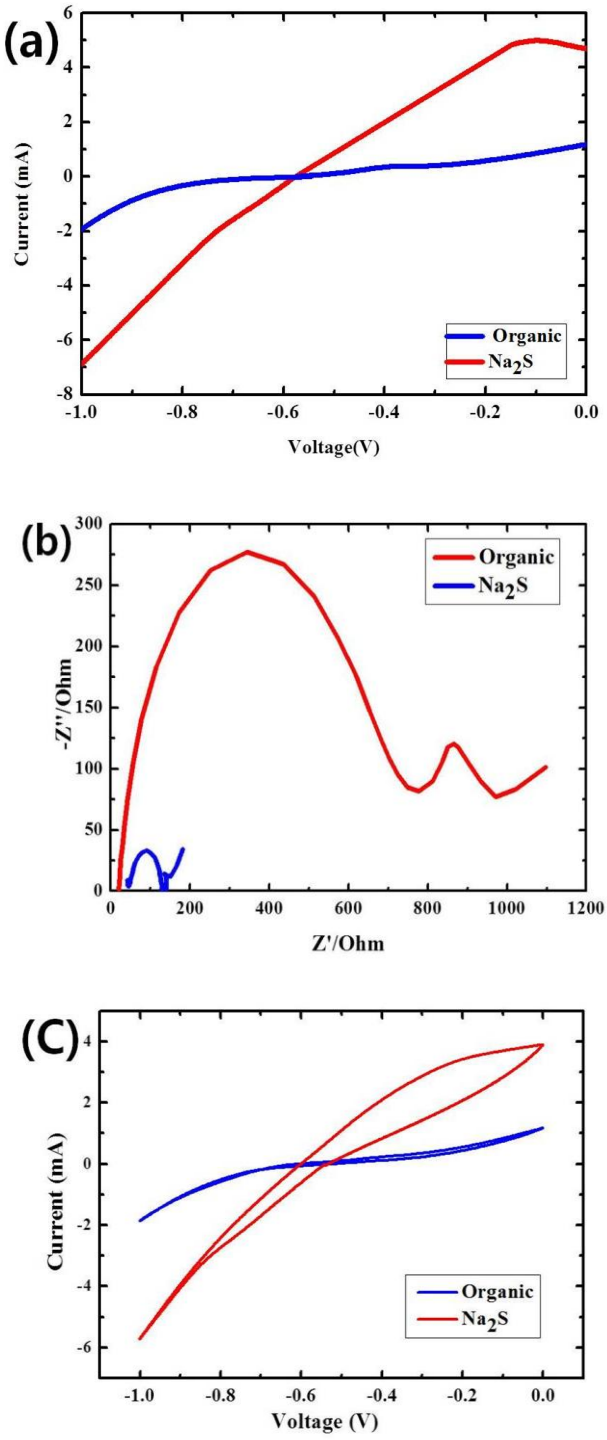


Fig 5.12 Electrochemical characterization of the counter electrode in a three electrode system with SCE used as reference (a) Linear sweep voltammetry of organic capped $Cu_2S$ and $Na_2S$ capped $Cu_2S$ in 2 M/2 M poly sulfide solution (b) Electrical impedance measurements of organic capped $Cu_2S$ and $Na_2S$ capped $Cu_2S$ on FTO substrates.

# 6. Conclusions

The CdSe nanoparticels based on the QDSSCs were tested under AM 1.5G one sun illumination function of a variety of counter electrode. $Cu_2S$ NCs used as counter electrode for increasing high catalytic activity and stability leads to a cell performance of Jsc=5.99mA/$cm^{-2}$ Voc=0.31V FF=0.40 and efficiency=0.8%, which is 0.2% higher than that of the Pt counter electrode. We also studied on the effects of nanomaterials and surface modification on the operation of QDSSCs using photoanode materials like CdSe synthesized by SILAS and hot-temperature injection method. The cell efficiency of QDSSCs based on the pre-synthesized colloidal CdSe nanoparticles showed about 0.42%, which was almost twice as low as that of SILAR method. The efficiency loss of photovoltaic performance was primarily due to the reduction of electron tunneling injection between QDs and electrode materials. The rate of reduction reaction of inorganic capped_$Cu_2S$ $NC_S$ counter electrode was confirmed through CV and LSV; it was three times much faster compared to organic capped $Cu_2S$ NCs. The use of new materials, surface treatments of photoanode and combined absorbers need to further explore and understand in improving the performance of QDSSCs.

# References


1. NREL sources.
2. Papageorgiou, N., et al., "The Performance and Stability of Ambient Temperature Molten Salts for Solar Cell Applications." *Journal of The Electrochemical Society*, 1996. 143(10): p. 3099-3108.
3. Kamat, P.V., "Meeting the Clean Energy Demand: Nanostructure Architectures for Solar Energy Conversion." *The Journal of Physical Chemistry C,* 2007. 111(7): p. 2834-2860.
4. Tvrdy, K. and P.V. Kamat, "Substrate Driven Photochemistry of CdSe Quantum Dot Films: Charge Injection and Irreversible Transformations on Oxide Surfaces†." *The Journal of Physical Chemistry A*, 2009. 113(16): p. 3765-3772.
5. Yu, W.W., et al., "Experimental Determination of the Extinction Coefficient of CdTe, CdSe, and CdS Nanocrystals." *Chemistry of Materials*, 2003. 15(14): p. 2854-2860.
6. Wang, P., et al., "Stable New Sensitizer with Improved Light Harvesting for Nanocrystalline Dye-Sensitized Solar Cells." *Advanced Materials*, 2004. 16(20): p. 1806-1811.
7. Schaller, R.D., et al., "Seven Excitons at a Cost of One: Redefining the Limits for Conversion Efficiency of Photons into Charge Carriers." *Nano Letters*, 2006. 6(3): p. 424-429.
8. Trinh, M.T., et al., "In Spite of Recent Doubts Carrier Multiplication Does Occur in PbSe Nanocrystals." *Nano Letters*, 2008. 8(6): p. 1713-1718.
9. Vogel, R., K. Pohl, and H. Weller, "Sensitization of highly porous, polycrystalline TiO2 electrodes by quantum sized CdS." *Chemical Physics Letters*, 1990. 174(3–4): p. 241-246.
10. Vogel, R., P. Hoyer, and H. Weller, "Quantum-Sized PbS, CdS, Ag2S, Sb2S3, and Bi2S3 Particles as Sensitizers for Various Nanoporous Wide-Bandgap Semiconductors." *The Journal of Physical Chemistry*, 1994. 98(12): p. 3183-3188.
11. Nikumbh, M., V. Gore, and R.B. Gore, "Structural, optical and photoelectrochemical studies of the cadmium sulphide films grown by chemical bath deposition." *Renewable Energy*, 1997. 11(4): p. 459-467.
12. Mane, R.S. and C.D. Lokhande, "Chemical deposition method for metal chalcogenide thin films." *Materials Chemistry and Physics*, 2000. 65(1): p. 1-31.
13. Kanniainen, T., et al., "Growth of lead selenide thin films by the successive ionic layer adsorption and

reaction (SILAR) technique." *Journal of Materials Chemistry*, 1996. 6(6): p. 983-986.

14. Nicolau, Y.F., "Solution deposition of thin solid compound films by a successive ionic-layer adsorption and reaction process." *Applications of Surface Science*, 1985. 22–23, Part 2(0): p. 1061-1074.
15. Robel, I., et al., "Quantum Dot Solar Cells. Harvesting Light Energy with CdSe Nanocrystals Molecularly Linked to Mesoscopic TiO2 Films." *Journal of the American Chemical Society*, 2006. 128(7): p. 2385-2393.
16. Lopez-Luke, T., et al., "Nitrogen-Doped and CdSe Quantum-Dot-Sensitized Nanocrystalline $TiO_2$ Films for Solar Energy Conversion Applications." *The Journal of Physical Chemistry C*, 2008. 112(4): p. 1282-1292.
17. Leschkies, K.S., et al., "Photosensitization of ZnO Nanowires with CdSe Quantum Dots for Photovoltaic Devices." *Nano Letters*, 2007. 7(6): p. 1793-1798.
18. Mora-Seró, I., et al., "Factors determining the photovoltaic performance of a CdSe quantum dot sensitized solar cell: the role of the linker molecule and of the counter electrode." *Nanotechnology*, 2008. 19(42): p. 424007.
19. Guijarro, N.s., et al., "CdSe Quantum Dot-Sensitized TiO2 Electrodes: Effect of Quantum Dot Coverage and Mode of Attachment." *The Journal of Physical Chemistry C*, 2009. 113(10): p. 4208-4214.
20. Radich, J.G., R. Dwyer, and P.V. Kamat, "Cu2S Reduced Graphene Oxide Composite for High-Efficiency Quantum Dot Solar Cells. Overcoming the Redox Limitations of S2–/Sn2– at the Counter Electrode." *The Journal of Physical Chemistry Letters*, 2011. 2(19): p. 2453-2460.
21. Chi, W.S., et al., "Employing electrostatic self-assembly of tailored nickel sulfide nanoparticles for quasi-solid-state dye-sensitized solar cells with Pt-free counter electrodes." *Chemical Communications*, 2012. 48(76): p. 9501-9503.
22. Lee, J.-S., et al., "Band-like transport, high electron mobility and high photoconductivity in all-inorganic nanocrystal arrays". *Nat Nano, 2011*. 6(6): p. 348-352.
23. NREL sources.
24. Brabec, C.D., "Bulk heterojunction solar cells." *J. MRS Bulletin*, 2008. 33: p. 670.
25. Schaller, R.D. and V.I. Klimov, "High Efficiency Carrier Multiplication in PbSe Nanocrystals: Implications for Solar Energy Conversion." *Physical Review Letters*, 2004. 92(18): p. 186601.
26. Henglein, A., "Photochemistry of colloidal cadmium sulfide. 2. Effects of adsorbed methyl viologen

and of colloidal platinum." *The Journal of Physical Chemistry*, 1982. 86(13): p. 2291-2293.

27. Semiconductor nanoparticles

28. Park, N.G., J. van de Lagemaat, and A.J. Frank, "Comparison of Dye-Sensitized Rutile- and Anatase-Based $TiO_2$ Solar Cells." *The Journal of Physical Chemistry B*, 2000. 104(38): p. 8989-8994.

29. Yasuhiro Tachibana1), H.Y.A., Yasuhide Ohtsuka1), Tsukasa Torimoto2), Susumu Kuwabata1) "CdS Quantum Dots Sensitized $TiO_2$ Sandwich Type Photoelectrochemical Solar Cells." *Chemistry Letters*, 2007. 36(1): p. 88-89.

30. Lee, H.J., et al., "Regenerative PbS and CdS Quantum Dot Sensitized Solar Cells with a Cobalt Complex as Hole Mediator." *Langmuir*, 2009. 25(13): p. 7602-7608.

31. Giménez, S., et al., "Improving the performance of colloidal quantum-dot-sensitized solar cells." *Nanotechnology*, 2009. 20(29): p. 295204.

32. Lee, Y.-L. and Y.-S. Lo, "Highly Efficient Quantum-Dot-Sensitized Solar Cell Based on Co-Sensitization of CdS/CdSe." *Advanced Functional Materials*, 2009. 19(4): p. 604-609.

33. Cahen, G.H.a.J.M.a.D., "Electrocatalytic Electrodes for the Polysulfide Redox System." *ELECTROCHEMICAL SCIENCE AND TECHNOLOGY*"' 1980. 127(3): p. 544-549.

34. Hagfeldt, A., et al., "Dye-Sensitized Solar Cells." *Chemical Reviews*, 2010. 110(11): p. 6595-6663.

35. Koide, N., et al., "Improvement of efficiency of dye-sensitized solar cells based on analysis of equivalent circuit." *Journal of Photochemistry and Photobiology A: Chemistry*, 2006. 182(3): p. 296-305.

36. Shaheen, S.E., et al., "2.5% efficient organic plastic solar cells." *Applied Physics Letters*, 2001. 78(6): p. 841-843.

37. Wu, Y., et al., "Synthesis and Photovoltaic Application of Copper(I) Sulfide Nanocrystals." *Nano Letters*, 2008. 8(8): p. 2551-2555.

38. Pernik, D.R., et al., Tracking the Adsorption and Electron Injection Rates of CdSe Quantum Dots on TiO2: Linked versus Direct Attachment. The Journal of Physical Chemistry C, 2011. 115(27): p. 13511-13519.

39. Lee, H., et al., "Efficient CdSe Quantum Dot-Sensitized Solar Cells Prepared by an Improved Successive Ionic Layer Adsorption and Reaction Process." *Nano Letters*, 2009. 9(12): p. 4221-4227.

40. Lee, W., et al., "Co-sensitization of vertically aligned TiO2 nanotubes with two different sizes of CdSe quantum dots for broad spectrum." *Electrochemistry Communications*, 2008. 10(10): p. 1579-1582.

41. Steigerwald, M.L., et al., "Surface derivatization and isolation of semiconductor cluster molecules." *Journal of the American Chemical Society*, 1988. 110(10): p. 3046-3050.

42. Bawendi, M.G., et al., "X-ray structural characterization of larger CdSe semiconductor clusters." *The Journal of Chemical Physics*, 1989. 91(11): p. 7282-7290.

# 요 약 문

## 양자점감응형 태양전지에 관한 연구

본 연구는 폴리설파이드계열의 전해질을 이용하는 양자점감응형 태양전지가 상대전극에 따라서 어떠한 특성을 내는지 살펴보았다. 기존의 염료감응형 태양전지에서는 상대전극으로 백금이 많이 이용되었다. 하지만 설파이드계열 전해질은 백금 표면에 화학적으로 흡착되기 때문에 장애물로 작용이 되어서 전해질의 환원반응을 방해한다. 이는 높은 과전압을 초래해서 효율에 악영향을 미친다.

이에 본 연구에서 나노입자를 이용한 상대전극을 제조방법을 이용했다. 우리는 먼저 황화구리(II) 나노입자를 합성한 후, 헥센과 옥테인이 들어있는 매직솔루션으로 분산한다. 그리고 FTO 기판에 뿌린 후 어닐링을 해서 사용했다. 이 방법을 이용하면 monolayer형태로 상대전극을 이용할 수 있었다.

그 결과 $Cu_2S$를 활용했을 때 Pt전극보다 0.2%가 상승하는 결과를 가져왔다. LSV결과를 통하여, 우리는 유기 리간드를 무기 리간드로 바꾸었을 때 환원반응의 속도가 3배정도 상승하는 것을 확인할 수 있었다. 또한 EIS결과를 통해서 저항이 더 줄어드는 것도 확인을 할 수 있었다. 하지만 실제 효율에서는 별 차이가 없었다. 태양전지의 효율 감소원인으로는 전자환원반응뿐만 아니라, 전자정공재결합도 관련되어 있어서라고 생각한다. 그리고 우리는 colloidal nanoparticles 방법을 이용해서 photoanode도 제작해보았다. 이 방법을 활용하면 크기와 모양을 정확하게 컨트롤 할 수 있다. 하지만 Colloidal nanoparticles을 통해서 셀을 제작하면 SILAR에 비해서 0.4%정도 낮다. 첫 번째인 이유는 흡수하는 영역의 차이로 인해서 발생할 수 있는 전하의 양이 다르다. 다른 이유로는 리간드로 인해서 콜로이달 방법을 사용하게 되면 추가적인 Separation이 발생될 우려가 있어서다.

핵심어: 양자점감응형 태양전지, 실라방법, 콜로이달 나노파티클 방법, 리간드변환, $Cu_2S$ 나노크리스탈